

Novel β - and γ -Amino Acid-Derived Inhibitors of Prostate-Specific Membrane Antigen

Kyul Kim, Hongmok Kwon, Cyril Barinka, Lucia Motlova, SangJin Nam, Doyoung Choi, Hyunsoo Ha, Hwanhee Nam, Sang-Hyun Son, Il Minn, Martin G. Pomper, Xing Yang,* Zsofia Kutil,* and Youngjoo Byun*



Cite This: <https://dx.doi.org/10.1021/acs.jmedchem.9b02022>



Read Online

ACCESS |



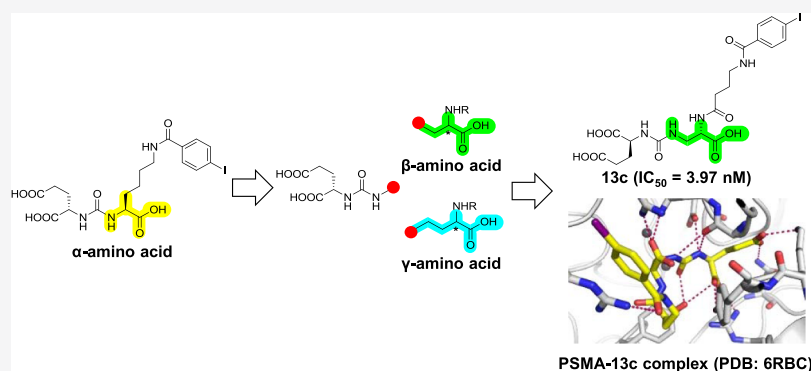
Metrics & More



Article Recommendations



Supporting Information



ABSTRACT: Prostate-specific membrane antigen (PSMA) is an excellent biomarker for the early diagnosis of prostate cancer progression and metastasis. The most promising PSMA-targeted agents in the clinical phase are based on the Lys–urea–Glu motif, in which Lys and Glu are α -(L)-amino acids. In this study, we aimed to determine the effect of β - and γ -amino acids in the S1 pocket on the binding affinity for PSMA. We synthesized and evaluated the β - and γ -amino acid analogues with (S)- or (R)-configuration with keeping α -(L)-Glu as the S1'-binding pharmacophore. The structure–activity relationship studies identified that compound 13c, a β -amino acid analogue with (R)-configuration, exhibited the most potent PSMA inhibitory activity with an IC_{50} value of 3.97 nM. The X-ray crystal structure of PSMA in complex with 13c provided a mechanistic basis for the stereochemical preference of PSMA, which can guide the development of future PSMA inhibitors.

INTRODUCTION

Prostate cancer (PCa) is the most commonly diagnosed cancer and the second leading cause of cancer-related deaths, only behind lung cancer in the United States.¹ Although the overall 5 year survival rate for patients with PCa in the United States is 97.3%, this drops drastically to 29% among patients with advanced stage PCa.¹ PCa usually shows no physical symptoms until it progresses to an advanced stage.² Hence, early and accurate diagnosis of PCa is critical for successful treatment. Prostate-specific membrane antigen (PSMA) is an attractive biomarker for the diagnosis of primary and metastatic PCa.³ PSMA is a type II integral membrane metalloprotease which shows restricted expression on the cell surface of prostate carcinomas, particularly in androgen-independent, advanced, and metastatic states.^{4,5} Furthermore, its expression levels positively correlate with tumor aggressiveness and metastasis.^{6,7}

There are many studies on the identification of PSMA-targeted small-molecule inhibitors.^{7–14} These small molecules are labeled with radionuclides for the imaging and therapy of PCa.^{7,8,15–18} In parallel with the discovery of PSMA inhibitors,

the X-ray crystal structures of PSMA in complex with small molecules have provided mechanistic insights into the binding modes in the active site.^{19–23} According to the PSMA crystal structures, the PSMA-active site consists of three distinct subpockets, including a “glutamate-sensor” S1' site (pharmacophore), a “zinc-binding” site, and an amphiphilic S1 site (nonpharmacophore). In particular, the structural freedom provided by the S1 site allows diverse structural modifications to PSMA inhibitors.^{20,24,25} Since the pioneering work by Kozikowski and colleagues,²⁶ the most common scaffold of PSMA inhibitors is a lysine–urea–glutamate (Lys–urea–Glu) motif that has a high binding affinity and specificity for PSMA despite the diverse structural variation in the P1 site. The ϵ -

Received: December 6, 2019

Published: February 25, 2020

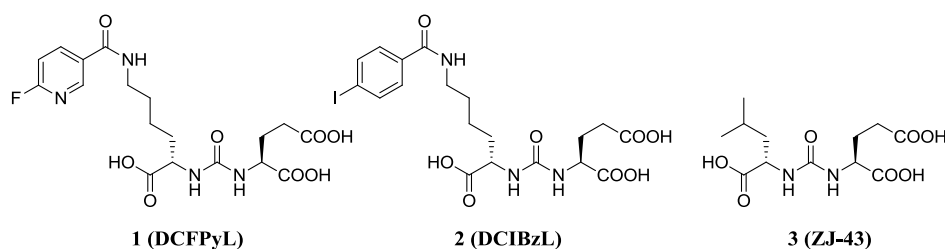
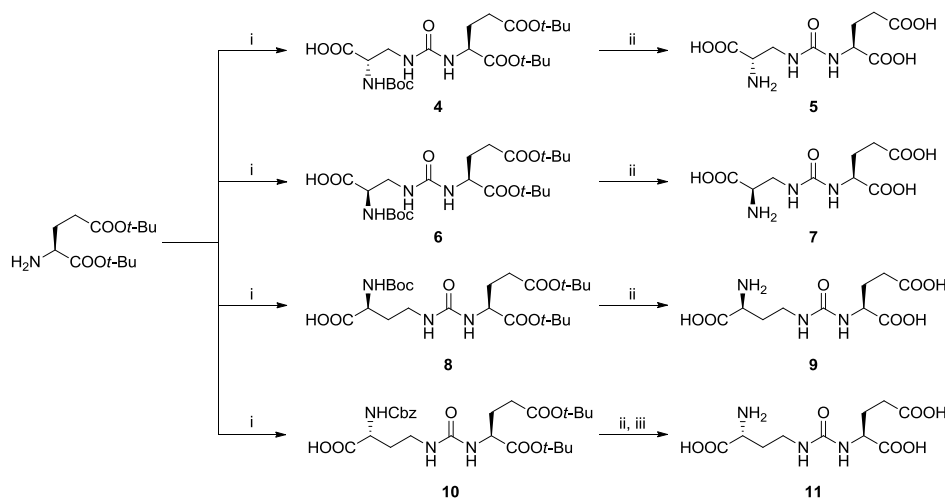


Figure 1. Representative α -(L)-amino acid PSMA inhibitors.

Scheme 1. Synthesis of Dipeptides Derived from β - and γ -Amino Acids^a



^aReagents and conditions: (i) triphosgene, Et₃N, CH₂Cl₂, -78 °C to rt, 30 min, and then (*S*)-3-amino-2-(Boc-amino)propanoic acid (for 4), (*R*)-3-amino-2-(Boc-amino)propanoic acid (for 6), (*S*)-4-amino-2-(Boc-amino)butanoic acid (for 8), and (*R*)-4-amino-2-(Cbz-amino)butanoic acid (for 10), rt, 24 h; (ii) TFA/CH₂Cl₂ (1/4, v/v), rt, 2 h; and (iii) 10% Pd/C, H₂, MeOH, 2 h.

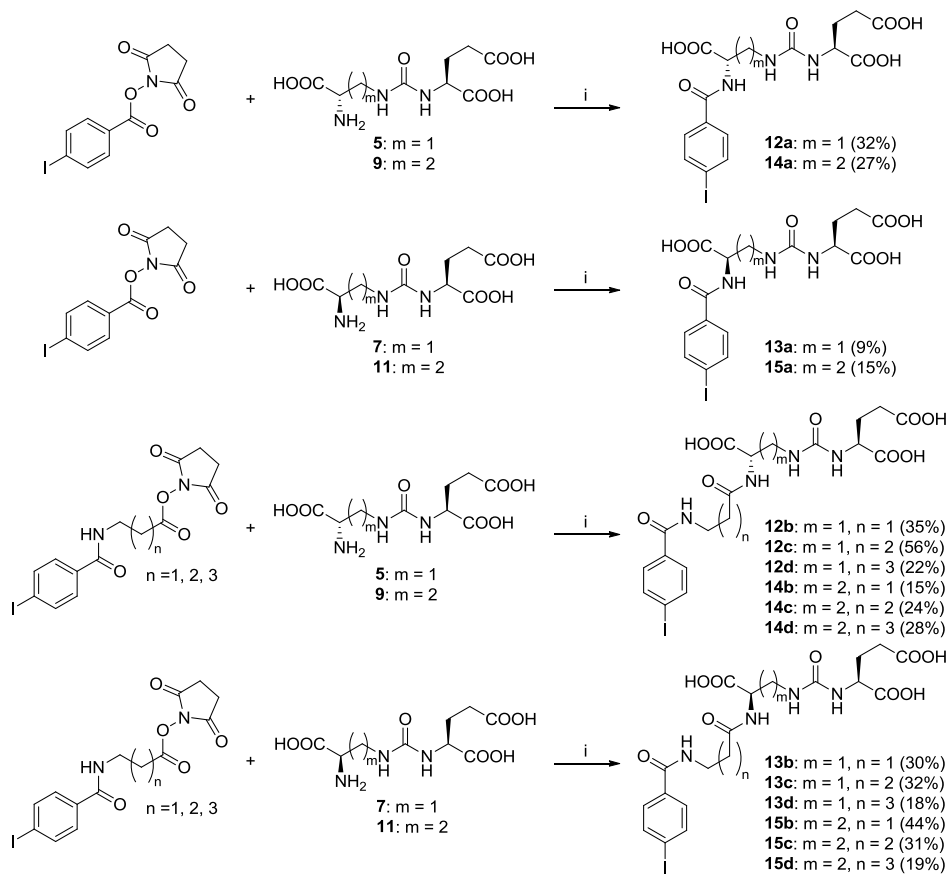
amine group of lysine in Lys–urea–Glu has been conjugated with a variety of imaging prosthetic groups and diverse linkers.^{27–31} Some excellent and comprehensive recent reviews on PSMA-targeted imaging probes derived from the Lys–urea–Glu motifs were reported.^{32–36}

Although diverse amino acids (e.g., Lys, Leu, and Cys) have been introduced to the P1 site, all of these are α -(L)-amino acids (Figure 1). The insertion of methylene (–CH₂–) or ethylene (–CH₂CH₂–) group between COOH and NH₂ in the P1 site was expected to enhance the conformational freedom. In addition, determining the relationship of PSMA binding affinity with the absolute configuration of β - and γ -amino acids will provide valuable information for understanding PSMA-targeted inhibitors in the P1 region. In this study, we aimed to investigate the effect of β - and γ -amino acids with (*S*)- or (*R*)-configuration in the S1 pocket on the binding affinity for PSMA. We synthesized and evaluated the β - and γ -amino acid analogues with (*S*)- or (*R*)-configuration and determined PSMA X-ray structures with the most potent β - and γ -amino acid inhibitors.

RESULTS AND DISCUSSION

The synthesis of β - and γ -amino acid PSMA inhibitors was accomplished by covalently attaching four different *p*-iodobenzoyl derivatives that varied in the length of the aliphatic spacer to urea-based β - and γ -amino acid dipeptide scaffolds with (*S*)- or (*R*)-configuration. In α -amino acid PSMA inhibitors, the *p*-iodobenzoyl group was located into the accessory pocket at the S1 site and interacted with the arginine patch region to contribute to strong PSMA binding.²⁰ The *p*-

iodobenzoyl group was also expected to increase the PSMA binding affinity in the β - and γ -amino acid PSMA inhibitors. The synthetic routes are shown in Schemes 1 and 2. The synthesis of the two diastereomeric pairs of Glu–urea– β -amino acid (5 and 7) and Glu–urea– γ -amino acid (9 and 11) was achieved in a two- or three-step protocol by coupling commercially available (*S*)-di-*tert*-butyl-glutamic acid with (*S*)- or (*R*)-3-amino-2-((*tert*-butoxycarbonyl)amino)propanoic acid and (*S*)- or (*R*)-4-amino-2-((*tert*-butoxycarbonyl)amino)butanoic acid, respectively. Briefly, (*S*)-di-*tert*-butyl-glutamic acid was treated with triphosgene under anhydrous conditions in the presence of triethylamine to afford the isocyanate intermediate, which reacted subsequently with the appropriate amino acids at room temperature to produce the protected four urea-based dipeptides (4, 6, 8, and 10). The *tert*-butoxycarbonyl (Boc) and *tert*-butyl ester (*Ot*-Bu) protecting groups of the dipeptides (4, 6, and 8) were removed by the treatment of 25% trifluoroacetic acid (TFA) solution in dichloromethane (DCM) to yield the urea-based dipeptides (5, 7, and 9), which were used for the next amide coupling reaction without further purification. However, the removal of the *tert*-butyl protecting groups of the dipeptide (10) with 25% TFA solution in DCM followed by the hydrogenation of the carboxybenzyloxy (Cbz) group using 10% Pd/C in the presence of H₂ gas in methanol afforded the urea-based dipeptide (11). The synthesis of four different *p*-iodobenzoyl derivatives was carried out via a three-step process using a previously established method (Supporting Information).^{37,38}

Scheme 2. Ring Extension and Variation of Carbon Chain Linker^a

^aReagents and conditions: (i) Et₃N, DMF, rt, and 2 h.

With four urea-based dipeptide scaffolds (**5**, **7**, **9**, and **11**) obtained, their assembly toward **12a–15d** was performed using *p*-iodobenzoyl derivatives with a variable length of the aliphatic part and activated *N*-hydroxysuccinimide (NHS) esters. Briefly, the Glu–urea– β -amino acid **5** with (*S*)-configuration was coupled with an aliphatic spacer having a different chain length in anhydrous *N,N*-dimethylformamide (DMF) using triethylamine as a base. The progress of the reaction was monitored by analytical high-performance liquid chromatography (HPLC) until the starting material disappeared completely. The crude product was purified by semipreparative HPLC to provide the final compounds (**12a–12d**) in moderate yield (22–56%) with high purity (>97%). The other β -amino acid analogues with (*R*)-configuration (**13a–13d**) and γ -amino acid analogues (**14a–14d** for (*S*) and **15a–15d** for (*R*)) were synthesized using a similar protocol.

To compare the change in lipophilicity based on the length of the linker and chirality, we used two different mobile phases [acetonitrile (ACN)/water and methanol/water] and determined the retention times of the synthesized compounds. As shown in Figure 2, compounds with longer linkers had a longer retention time than those with shorter linkers in all series. However, the γ -amino acid analogues (**14b** and **15b**), which had the ethylene spacer, eluted earlier than the corresponding analogues (**14a** and **15a**), which directly conjugated with the 4-iodobenzoyl group (Figure 2), irrespective of the mobile mixtures (CH₃CN/H₂O or CH₃OH/H₂O).

The PSMA inhibitory activities of the synthesized 16 inhibitors were determined by applying the fluorescence-based

NAALADase assay.^{39,40} We used extracts of the LNCaP cell line, which is an androgen-sensitive human prostate adenocarcinoma cell line that overexpresses PSMA. DCFPyL (**1**),²⁷ a known potent inhibitor of PSMA, was used as the positive control. Table 1 summarizes the IC₅₀ values of the synthesized PSMA inhibitors and compound **1**. The β -amino acid analogues (**13a–13d**) with (*R*)-configuration exhibited strong PSMA inhibitory activities with IC₅₀ values from 3.97 to 16.7 nM. However, the corresponding (*S*)-analogues were inactive (>1 μ M) except compound **12d** (155 nM). Compound **13c**, with a propylene spacer, was the most potent out of the β -amino acid inhibitors, with an IC₅₀ value of 3.97 nM. In the case of γ -amino acid analogues, the (*S*)-analogues (**14a–14d**) were more potent than the (*R*)-analogues (**15a–15d**). Compound **14b** (107 nM), with an ethylene linker, displayed the strongest PSMA inhibition in the γ -amino acid series but was less potent than **13c**.

To investigate the effect of α -amino acid stereochemistry on the P1 region, compound **17**, the diastereomer of DCIBzL (**2**),⁴¹ the most potent PSMA inhibitor based on the Lys–urea–Glu scaffold, was prepared as described in Scheme 3. By modifying the synthetic method for compound **2**, compound **17** was synthesized in three steps from commercial (*S*)-di-*tert*-butyl-glutamic acid and (*R*)-*tert*-butyl-lysine. Analytical HPLC studies showed a slight difference in retention time (5.59 min for **2** and 5.84 min for **17**) (see the Supporting Information). In vitro PSMA inhibitory studies showed a dramatic difference of IC₅₀ values (0.22 nM for **2** and 1.7 μ M for **17**), which indicated that the (*S*)-configuration in α -amino acids on the P1 region is critical for PSMA binding affinity. Previously, a significant

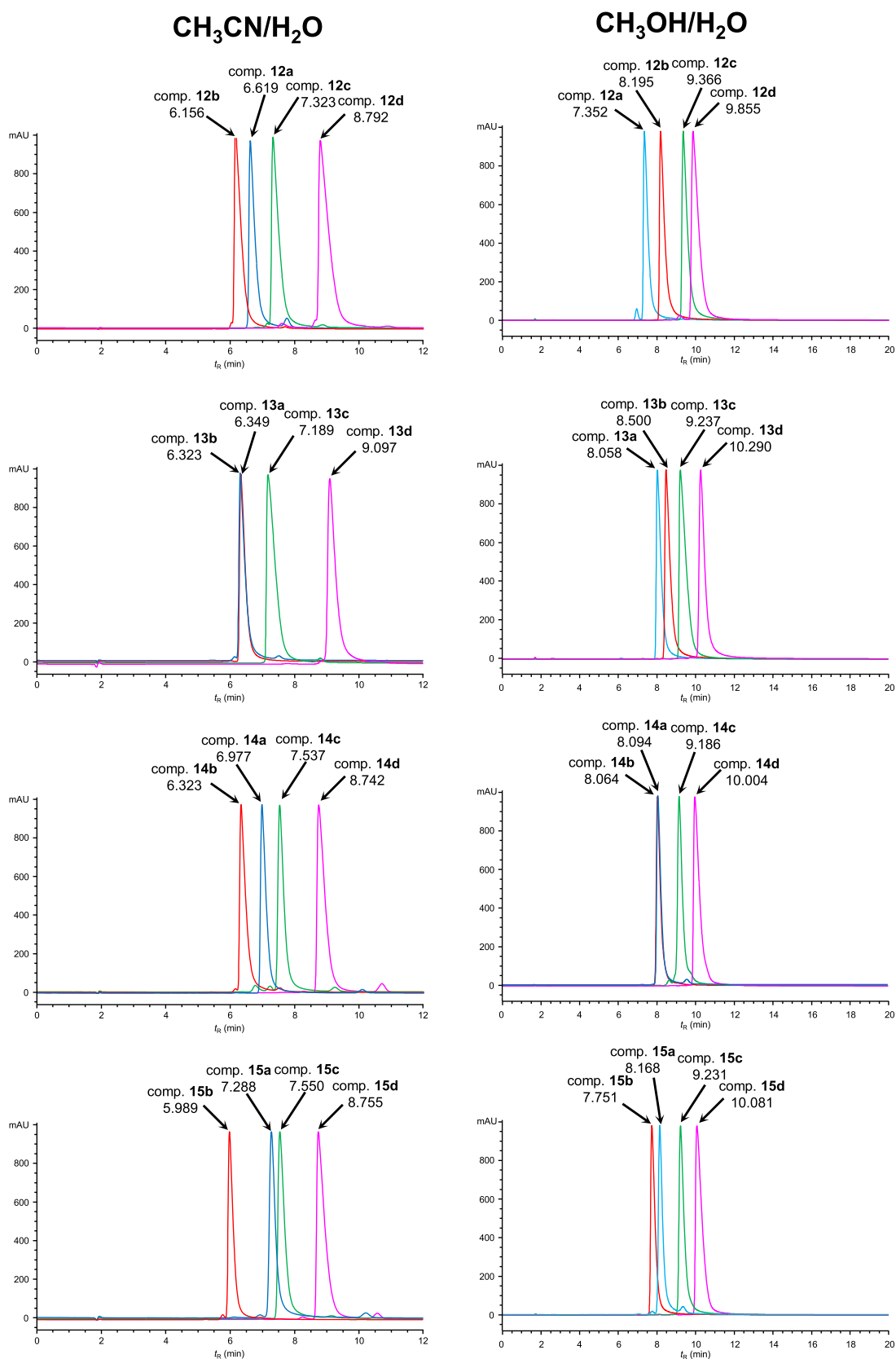
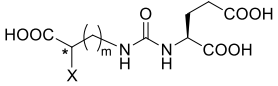


Figure 2. HPLC chromatograms of 16 compounds in two different eluent conditions. (a) ACN and water (25:75, v/v, and 0.1% FA), flow rate: 1 mL/min and (b) methanol and water (50:50, v/v, and 0.1% FA), flow rate: 0.7 mL/min.

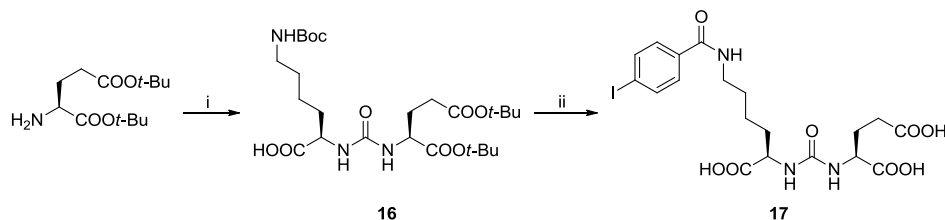
decrease in the PSMA inhibitory activity was observed when the (*S*)-leucine of ZJ-43 (**3**)⁴² on the P1 region was replaced with (*R*)-leucine that is consistent with our result.⁴³

To elucidate the importance of the absolute configuration and spacer length of β - and γ -amino acid inhibitors on their potency toward PSMA, we determined the crystal structures of human

Table 1. In Vitro PSMA-inhibitory Activity of the Synthesized Compounds



comp.	configuration	<i>m</i>	X	IC ₅₀ (nM)	95% CI ^a
DCFPyL (1)				1.56	0.38–6.32
12a	(S)	1	4-IC ₆ H ₄ CONH–	>1000	
12b	(S)	1	4-IC ₆ H ₄ CONH(CH ₂) ₂ CONH–	>1000	
12c	(S)	1	4-IC ₆ H ₄ CONH(CH ₂) ₃ CONH–	>1000	
12d	(S)	1	4-IC ₆ H ₄ CONH(CH ₂) ₄ CONH–	155	90.5–268
13a	(R)	1	4-IC ₆ H ₄ CONH–	11.0	6.63–18.1
13b	(R)	1	4-IC ₆ H ₄ CONH(CH ₂) ₂ CONH–	11.9	7.40–19.0
13c	(R)	1	4-IC ₆ H ₄ CONH(CH ₂) ₃ CONH–	3.97	2.47–6.36
13d	(R)	1	4-IC ₆ H ₄ CONH(CH ₂) ₄ CONH–	16.7	10.8–25.7
14a	(S)	2	4-IC ₆ H ₄ CONH–	399	140–1130
14b	(S)	2	4-IC ₆ H ₄ CONH(CH ₂) ₂ CONH–	107	66.8–1700
14c	(S)	2	4-IC ₆ H ₄ CONH(CH ₂) ₃ CONH–	284	163–494
14d	(S)	2	4-IC ₆ H ₄ CONH(CH ₂) ₄ CONH–	195	110–346
15a	(R)	2	4-IC ₆ H ₄ CONH–	>1000	
15b	(R)	2	4-IC ₆ H ₄ CONH(CH ₂) ₂ CONH–	>1000	
15c	(R)	2	4-IC ₆ H ₄ CONH(CH ₂) ₃ CONH–	>1000	
15d	(R)	2	4-IC ₆ H ₄ CONH(CH ₂) ₄ CONH–	>1000	
DCIBzL (2)	(S)	0	4-IC ₆ H ₄ CONH(CH ₂) ₄ –	0.22	0.17–0.30
17	(R)	0	4-IC ₆ H ₄ CONH(CH ₂) ₄ –	>1000	

^aConfidence interval.Scheme 3. Synthesis of Compound 17^a

^aReagents and conditions: (i) triphosgene, Et₃N, CH₂Cl₂, –78 °C to rt, 30 min, and then N^ε-Boc-D-lysine and (ii) TFA/CH₂Cl₂ (1/4, v/v), rt, 2 h, and then *N*-succinimidyl 4-iodobenzoate, Et₃N, DMF, rt, 2.5 h.

PSMA in complex with **13c** (β -amino acid) and **14b** (γ -amino acid) to the final resolution of 1.77 and 1.76 Å, respectively (Table 2). The Glu moiety of both inhibitors occupies the customary position in the S1' pocket, identical to the position in a published study on PSMA/urea-based inhibitor complexes (Figure 3).²⁰ The urea carbonyl oxygen atoms of **13c** and **14b** interact with the zinc(II) ion at a distance of 2.29 and 2.44 Å, respectively. The divergence among the binding modes of **13c**, **14b**, and **2** (PDB code 3D7H) becomes, however, apparent on their nonprime S1 side. The interactions between the P1 residues and the α -carboxylate of the Lys–urea–Glu scaffold have been shown to be critical for the high affinity of PSMA inhibitors, and the typical interaction pattern involves three direct and one water-mediated contacts with Arg534 and Arg536 comprising the P1 arginine patch.⁴⁴ In the case of **13c**, the P1 β -(*R*)-carboxylate interacts with the side chain of Arg534, forming one direct (2.7 Å) and one water-mediated (2.5 Å) hydrogen bond (Figure 4). For **14b**, the P1 γ -(*S*)-carboxylate forms a direct hydrogen bond with Arg536 (2.7 Å) and water-mediated hydrogen bonds with Arg534 (2.7 and 2.9 Å, respectively). Interestingly, both the P1 β - and γ -carboxylates of **13c** and **14b**, respectively, also form hydrogen bonds with the carbonyl/amide groups of the linker and can, in principle,

constrain the positioning of the distal *p*-iodobenzoyl moiety. It should be noted that changing the absolute configuration at the carbon atom bearing the nonprime carboxylate of **13c** and **14b** to (*S,S*) and (*R,S*) diastereomers, respectively, would place the P1 carboxylate groups in unfavorable positions. In the case of **13c**, the change in chirality made it too close to the *p*-iodobenzoyl group that was presumably the cause of its displacement (Supporting Information). In the case of **14b**, the change in chirality forced the *p*-iodobenzoyl group away from the arginine patch (Supporting Information), resulting in the loss of critical interactions.⁴⁴ These results provide a mechanistic rationale for the measured inhibition constants where the changes in the absolute configuration at the side carbon atoms decreased inhibition constants by more than 250-fold (Table 1). It should be noted that the *p*-iodobenzoyl group in the β - and γ -amino acid PSMA inhibitors may interact with human serum albumin and affect the biodistribution of the parent compound, which was observed with the α -amino acid PSMA inhibitors.⁴⁵

The distal *p*-iodobenzoyl groups of both **13c** and **14b** are placed inside the accessory hydrophobic pocket formed by the opening of the arginine patch as reported previously.^{20,44} Although the *p*-iodobenzoyl ring of **13c** overlaps well with the

Table 2. Data Collection and Refinement Statistics

data collection statistics		
inhibitor	13c	14b
PDB ID	6RBC	6S1X
space group	I222	I222
unit cell parameters <i>a</i> , <i>b</i> , <i>c</i> (Å)	101.5, 130.5, 159.0	101.4, 130.2, 159.3
wavelength (Å)	0.9184	0.9184
resolution limits (Å)	50–1.77 (1.88–1.77)	50–1.76 (1.86–1.76)
no. of unique refl.	102,705 (16,397)	104,162 (16,420)
redundancy	6.7 (6.5)	6.0 (5.7)
completeness (%)	99.9 (99.3)	99.6 (98.4)
<i>I</i> / σ (<i>I</i>)	14.5 (1.94)	15.91 (1.92)
<i>R</i> _{merge}	0.083 (0.827)	0.072 (0.823)
refinement statistics		
resolution limits (Å)	45.00–1.77 (1.81–1.77)	45.00–1.76 (1.80–1.76)
total number of reflections	100,601 (7450)	102,046 (7427)
number of reflections in a working set	985,00 (7297)	99,947 (7277)
number of reflections in a test set	2101 (153)	2099 (150)
<i>R</i> / <i>R</i> _{free} (%)	16.5/19.1 (27.0/27.2)	16.8/19.4 (33.3/34.9)
total number of non-H atoms	6603	6776
number of non-H atoms	5802	5968
number of inhibitor molecules	1	1
number of water molecules	601	572
average <i>B</i> -factor (Å ²)	35.65	37.29
protein	34.41	35.93
water molecules	43.60	44.55
inhibitor	32.60	39.8
Ramachandran plot (%)		
most favored	97%	96%
additionally allowed	3%	3%
disallowed	0%	1%
rms deviations:		
bond lengths (Å)	0.011	0.012
bond angles (deg)	1.73	1.74
chiral centers (Å ³)	0.12	0.12

“canonical” position observed for (α)-Lys–urea–Glu molecules comprising the P1 lysine linker, such as compound **2**,²⁰ the *p*-iodobenzoyl moiety of **14b** is shifted by 1.4 Å and rotated by approximately 45°. Concurrently, the side chain of Arg463, which forms the “upper” wall of the accessory hydrophobic pocket, is pushed away by 2.1 Å to accommodate the rotated *p*-iodobenzoyl ring. Structurally, the placement of the *p*-iodobenzoyl ring of **14b** into the “canonical”, and presumably energetically favorable, position is sterically prohibited by the position of the P1 γ -carboxylate. These observations imply that, in general, when the *p*-iodobenzoyl ring is to be used as the distal moiety anchoring the inhibitor at the accessory hydrophobic pocket, the γ -amino acid analogues may be excluded because of their positional incompatibility. This is demonstrated by the fact that the “preferred” (*S*)-analogues of γ -amino acid are overall less potent than the “preferred” (*R*)-analogues of the β -amino acid analogues (Table 1).

The $F_o - F_c$ electron density map for the distal part (the linker and the *p*-iodobenzoyl group) of **14b** is much weaker compared to the rest of the compound, suggesting its positional variability and the existence of several (at least two) alternative conformations (although these cannot be modeled because of the absence of strong positive $F_o - F_c$ electron density peaks).

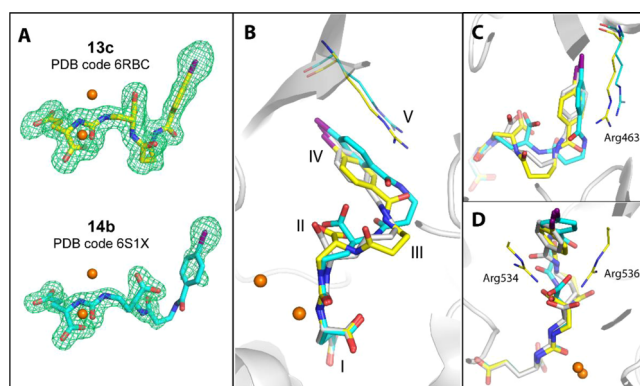


Figure 3. (A) $F_o - F_c$ difference maps (green) for **13c** (PDB ID: 6RBC) and **14b** (PDB ID: 6S1X) are contoured at 3.0 σ and modeled inhibitors are shown in stick representation with atoms colored in yellow and cyan (carbons of **13c** and **14b**, respectively), red (oxygen), blue (nitrogen), and magenta (iodine). The active site zinc ions are shown as orange spheres. (B–D) Comparison of binding modes of **13c** and **14b** with DCIBzL (gray carbons) from three different view angles, while the position of the urea–Glu moiety in the S1' pocket is identical in all cases (I), the positioning of the linkers (III) and the interaction pattern of the P1 carboxylate groups with Arg534 and Arg536 of the arginine patch differ substantially (II). The rotation of the *p*-iodobenzoyl group of **14b** (IV) results in the displacement of Arg463 (V).

We speculate that in addition to the binding modeled for **14b**, the distal *p*-iodobenzoyl moiety in alternative binding mode(s) is placed outside the accessory hydrophobic pocket in the internal funnel. As the engagement of the accessory hydrophobic pocket by the *p*-iodobenzoyl group contributes to higher inhibitor affinity by the avidity effect, its displacement into the internal funnel can result in a weaker affinity for PSMA, as demonstrated in our inhibition experiments (Table 1). The PSMA affinity of the most potent derivative **13c** is approximately 18-fold lower compared to the parent DCIBzL compound (Table 1). However, the inhibitory potency of **13c** is in a similar range as that of the PSMA-specific ligand **1** used in clinical trial (3.97 vs 1.56 nM). Consequently, upon radiolabeling, the new compounds reported here can be in principle used as diagnostic agents of PCa in vivo.

CONCLUSIONS

We designed and synthesized novel dipeptide urea-based PSMA inhibitors which possess β - and γ -amino acids with (*S*)- or (*R*)-configuration on the P1 side. According to the structure–activity relationship studies, the β -amino acid analogues with (*R*)-configuration inhibited PSMA stronger than the corresponding analogues with (*S*)-configuration, whereas the γ -amino acids with (*S*)-configuration were more active than the corresponding ones with (*R*)-configuration. The β -amino acid compound with (*R*)-configuration, **13c**, exhibited the strongest PSMA inhibitory activity in this series with an IC_{50} value of 3.97 nM. Hydrogen-bonding interactions with the arginine patch and proper placement of the *p*-iodobenzoyl ring in the accessory hydrophobic pocket were observed in the X-ray crystal structure, which explains the strong affinity of **13c** for PSMA. Compound **13c** has the potential to be a prototype molecule for the development of new β -amino acid PSMA inhibitors.

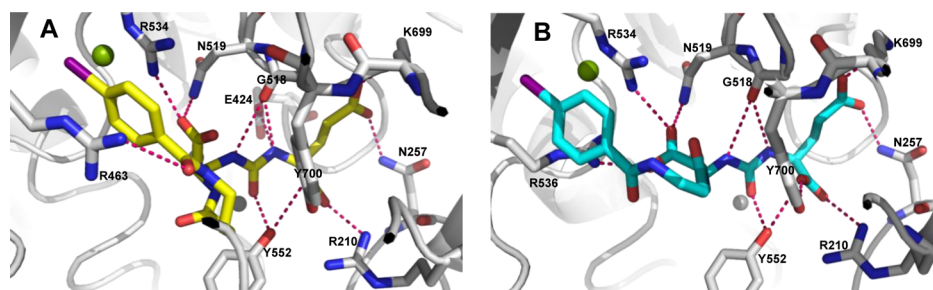


Figure 4. (A) PSMA represented with its active site (PDB ID: 6RBC) cocrystallized with **13c** (yellow) and (B) PSMA represented with its active site (PDB ID: 6S1X) cocrystallized with **14b** (light blue).

EXPERIMENTAL SECTION

General. All the chemicals and solvents used in the reaction were purchased from Sigma-Aldrich, TCI, or Alfa Aesar and were used without further purification. The reactions were monitored by TLC on 0.25 mm Merck precoated silica gel plates (60 F₂₅₄). The reaction progress was monitored by TLC analysis using a UV lamp and/or KMnO₄ staining for detection purposes. Column chromatography was performed on silica gel (230–400 mesh, Merck, Darmstadt, Germany). ¹H and ¹³C NMR spectra were recorded at room temperature (298 K) in CDCl₃ (7.26/77.16 ppm), CD₃CN (1.94/118.26 ppm), D₂O (4.79 ppm), CD₃OD (3.31/49.00 ppm), or (CD₃)₂SO (2.50/39.52 ppm) on either a Bruker BioSpin AVANCE 300 MHz NMR or a Bruker Ultrashield 600 MHz Plus spectrometer and referenced to an internal solvent. Chemical shifts are reported in parts per million (ppm). Coupling constants (*J*) are given in hertz. Splitting patterns are indicated as s, singlet; d, doublet; t, triplet; q, quartet; m, multiplet; and br, broad for ¹H NMR data. High-resolution mass spectroscopy (HRMS) spectra were recorded on an Agilent 6530 Accurate mass Q-TOF LC/MS spectrometer. Low-resolution mass spectroscopy analyses were performed from an API 150EX ESI-MS spectrometer. HPLC purification was performed on an Agilent 1260 Infinity (Agilent). The purification of synthesized compounds was performed by semipreparative reverse-phase HPLC (RP-HPLC; Agilent 1260 series HPLC instrument) using a semipreparative column (Phenomenex Gemini-NX C18, 110 Å, 150 mm × 10 mm, 5 μm) over 30 min at a flow rate of 2 mL/min. A suitably adjusted gradient of 5% B to 95% B was used, where solvent A was 0.1% formic acid (FA) in H₂O and solvent B was 0.1% FA in ACN. UV detection was carried out at 220 and 254 nm. The structural identification of each HPLC fractions was carried out by an electrospray ionization PE Biosystems SciexApi 150 EX mass spectrometer single quadrupole equipped with a turbo ion spray interface. The purity of all final compounds was measured by analytical RP-HPLC on an Agilent 1260 Infinity (Agilent) with a C18 column (Phenomenex, 150 mm × 4.6 mm, 3 μm, 110 Å). RP-HPLC was performed on two different solvent systems using the following isocratic conditions: for method A, the mobile phase was ACN and water (25:75, v/v, 0.1% FA); for method B, the mobile phase was methanol and water (50:50, v/v, 0.1% FA). All compounds were eluted with a flow rate of 1.0 mL/min (method A) or 0.7 mL/min (method B) and monitored using a UV detector: 254 nm. The purity of the tested compounds was >97%.

Synthesis. *(S)*-2-((*tert*-Butoxycarbonyl)amino)-3-(3-((*S*)-1,5-di-*tert*-butoxy-1,5-dioxopentan-2-yl)ureido)propanoic Acid (**4**). *L*-Glutamic acid di-*tert*-butyl ester hydrochloride (888 mg, 3.10 mmol) was placed in an oven-dried 100 mL two-necked round-bottom flask that was then fitted with a rubber septum and three-way connected to a balloon filled with argon. The flask was flushed with argon and anhydrous DCM (10 mL) was added, followed by triethylamine (3.5 mL, 24.5 mmol). After the mixture was cooled to −78 °C, triphosgene (303 mg, 1.02 mmol) in anhydrous DCM (5 mL) was added dropwise to the mixture. The reaction mixture was slowly warmed up to room temperature and stirred for 30 min. A solution of (*S*)-3-amino-2-(Boc-amino)propanoic acid (500 mg, 2.45 mmol) in anhydrous DCM (10 mL) and triethylamine (2.9 mL, 20.4 mmol) was added to the reaction mixture. The reaction mixture was stirred at room temperature for 24 h.

The reaction was quenched with ice-cooled 1 N HCl and extracted with DCM (ca. 100 mL × 3). The combined organic layer was dried over MgSO₄ and concentrated under reduced pressure. (*S*)-2-((*tert*-Butoxycarbonyl)amino)-3-(3-((*S*)-1,5-di-*tert*-butoxy-1,5-dioxopentan-2-yl)ureido)propanoic acid **4** (616 mg, 1.3 mmol) was obtained and used for the next steps without further purification.

(S)-2-(3-((*S*)-2-Amino-2-carboxyethyl)ureido)pentanedioic Acid (**5**). (*S*)-2-((*tert*-Butoxycarbonyl)amino)-3-(3-((*S*)-1,5-di-*tert*-butoxy-1,5-dioxopentan-2-yl)ureido)propanoic acid **4** (616 mg, 1.3 mmol) was dissolved in anhydrous DCM (8 mL), and TFA (2 mL) was slowly added at 0 °C. The reaction mixture was stirred at room temperature for 2 h. The reaction mixture was diluted with DCM and poured into iced water. The organic layer was washed with water and brine. The combined organic phase was dried over MgSO₄ and concentrated under reduced pressure. (*S*)-2-(3-((*S*)-2-Amino-2-carboxyethyl)ureido)pentanedioic acid **5** was obtained and used for the next steps without further purification.

(R)-2-((*tert*-Butoxycarbonyl)amino)-3-(3-((*S*)-1,5-di-*tert*-butoxy-1,5-dioxopentan-2-yl)ureido)propanoic Acid (**6**). *L*-Glutamic acid di-*tert*-butyl ester hydrochloride (870 mg, 3.0 mmol) was placed in an oven-dried 100 mL two-necked round-bottom flask that was then fitted with a rubber septum and three-way connected to a balloon filled with argon. The flask was flushed with argon and anhydrous DCM (10 mL) was added, followed by triethylamine (3.3 mL, 23.7 mmol). After the mixture was cooled to −78 °C, triphosgene (293 mg, 1.00 mmol) in anhydrous DCM (5 mL) was added dropwise to the mixture. The reaction mixture was slowly warmed up to room temperature and stirred for 30 min. A solution of (*R*)-3-amino-2-(Boc-amino)propanoic acid (500 mg, 2.45 mmol) in anhydrous DCM (10 mL) and triethylamine (2.9 mL, 20.4 mmol) was added to the reaction mixture. The reaction mixture was stirred at room temperature for 24 h. The reaction was quenched with ice-cooled 1 N HCl and extracted with DCM (ca. 100 mL × 3). The combined organic layer was dried over MgSO₄ and concentrated under reduced pressure. (*R*)-2-((*tert*-Butoxycarbonyl)amino)-3-(3-((*S*)-1,5-di-*tert*-butoxy-1,5-dioxopentan-2-yl)ureido)propanoic acid **6** was obtained and used for the next steps without further purification.

(S)-2-(3-((*R*)-2-Amino-2-carboxyethyl)ureido)pentanedioic Acid (**7**). (*R*)-2-((*tert*-Butoxycarbonyl)amino)-3-(3-((*S*)-1,5-di-*tert*-butoxy-1,5-dioxopentan-2-yl)ureido)propanoic acid **6** (1.19 g, 2.4 mmol) was dissolved in anhydrous DCM (8 mL), and TFA (2 mL) was slowly added at 0 °C. The reaction mixture was stirred at room temperature for 2 h. The reaction mixture was diluted with DCM and poured into iced water. The organic layer was washed with water and brine. The combined organic phase was dried over MgSO₄ and concentrated under reduced pressure. (*S*)-2-(3-((*R*)-2-Amino-2-carboxyethyl)ureido)pentanedioic acid **7** was obtained and used for the next steps without further purification.

(S)-2-((*tert*-Butoxycarbonyl)amino)-4-(3-((*S*)-1,5-di-*tert*-butoxy-1,5-dioxopentan-2-yl)ureido)butanoic Acid (**8**). *L*-Glutamic acid di-*tert*-butyl ester hydrochloride (820 mg, 2.8 mmol) was placed in an oven-dried 100 mL two-necked round-bottom flask that was then fitted with a rubber septum and three-way connected to a balloon filled with argon. The flask was flushed with argon and anhydrous DCM (10 mL) was added, followed by triethylamine (3.1 mL, 22.2 mmol). After the

mixture was cooled to $-78\text{ }^{\circ}\text{C}$, triphosgene (280 mg, 0.95 mmol) in anhydrous DCM (3 mL) was added dropwise to the mixture. The reaction mixture was slowly warmed up to room temperature and stirred for 30 min. A solution of (*S*)-4-amino-2-((*tert*-butoxycarbonyl)-amino)butanoic acid (500 mg, 2.3 mmol) in anhydrous DCM (5 mL) and triethylamine (2.5 mL, 17.9 mmol) was added to the reaction mixture. The reaction mixture was stirred at room temperature for 24 h. The reaction was quenched with ice-cooled 1 N HCl and extracted with DCM (ca. 100 mL \times 3). The combined organic layer was dried over MgSO_4 and concentrated under reduced pressure. (*S*)-2-((*tert*-butoxycarbonyl)amino)-4-(3-((*S*)-1,5-di-*tert*-butoxy-1,5-dioxopentan-2-yl)ureido)butanoic acid **8** was obtained and used for the next steps without further purification.

(*S*)-2-(3-((*S*)-3-Amino-3-carboxypropyl)ureido)pentanedioic Acid (**9**). (*S*)-2-((*tert*-butoxycarbonyl)amino)-4-(3-((*S*)-1,5-di-*tert*-butoxy-1,5-dioxopentan-2-yl)ureido)butanoic acid **8** (1.12 g, 2.4 mmol) was dissolved in anhydrous DCM (8 mL), and then, TFA (2 mL) was slowly added at $0\text{ }^{\circ}\text{C}$. The reaction mixture was stirred at room temperature for 2 h. The reaction mixture was diluted with DCM and poured into iced water. The organic layer was washed with water, followed by brine. The combined organic phase was dried over MgSO_4 and concentrated under reduced pressure. (*S*)-2-(3-((*S*)-3-Amino-3-carboxypropyl)ureido)pentanedioic acid **9** was obtained and used for the next steps without further purification.

(*R*)-2-(((Benzyloxy)carbonyl)amino)-4-(3-((*S*)-1,5-di-*tert*-butoxy-1,5-dioxopentan-2-yl)ureido)butanoic Acid (**10**). *L*-Glutamic acid di-*tert*-butyl ester hydrochloride (280 mg, 0.95 mmol) was placed in an oven-dried 100 mL two-necked round-bottom flask that was then fitted with a rubber septum and three-way connected to a balloon filled with argon. The flask was flushed with argon and anhydrous DCM (5 mL) was added, followed by triethylamine (1.0 mL, 7.60 mmol). After the mixture was cooled to $-78\text{ }^{\circ}\text{C}$, triphosgene (303 mg, 1.02 mmol) in anhydrous DCM (5 mL) was added dropwise to the mixture.

The reaction mixture was slowly warmed up to room temperature and stirred for 30 min. A solution of (*R*)-4-amino-2-(((benzyloxy)carbonyl)amino)butanoic acid (200 mg, 0.79 mmol) in anhydrous DCM (5 mL) and triethylamine (880 μL , 6.30 mmol) was added to the reaction mixture. The reaction mixture was stirred at room temperature for 24 h. The reaction was quenched with ice-cooled 1 N HCl and extracted with DCM (ca. 100 mL \times 3). The combined organic layer was dried over MgSO_4 and concentrated under reduced pressure. (*R*)-2-(((Benzyloxy)carbonyl)amino)-4-(3-((*S*)-1,5-di-*tert*-butoxy-1,5-dioxopentan-2-yl)ureido)butanoic acid **10** was obtained and used for the next steps without further purification.

(*S*)-2-(3-((*R*)-3-Amino-3-carboxypropyl)ureido)pentanedioic Acid (**11**). The crude product dissolved in MeOH (10 mL) was added to a catalytic amount of AcOH and hydrogenated in a Paar hydrogenation apparatus by using 10% Pd/C under hydrogen gas (40 psi). The reaction mixture was filtered through a pad of Celite, and the Celite pad was washed with MeOH. The filtrate was concentrated in vacuo.

To a solution of the intermediate in anhydrous DCM (8 mL), TFA (2 mL) was added dropwise at $0\text{ }^{\circ}\text{C}$. The reaction mixture was stirred vigorously at room temperature for 2 h. The reaction mixture was diluted with DCM and poured into iced water. The organic layer was washed with water and brine. The combined organic phase was dried over MgSO_4 and concentrated under reduced pressure. (*S*)-2-(3-((*R*)-3-Amino-3-carboxypropyl)ureido)pentanedioic acid **11** was obtained and used for the next steps without further purification.

Typical Procedure for the Synthesis of (*S*)-2-(3-((*S*)-2-Carboxy-2-(4-iodobenzamido)ethyl)ureido)pentanedioic Acid (12a**).** *N*-Succinimidyl 4-iodobenzoate (270 mg, 0.78 mmol) and (*S*)-2-(3-((*S*)-2-amino-2-carboxyethyl)ureido)pentanedioic acid **5** (175 mg, 0.63 mmol) were placed in an oven-dried 100 mL two-necked round-bottom flask that was then fitted with a rubber septum and three-way connected to a balloon filled with argon. The flask was flushed with argon and anhydrous DCM (2 mL) was added, followed by triethylamine (700 μL , 5.05 mmol). The reaction mixture was stirred at room temperature for 2 h. The reaction mixture was filtered through a 0.45 μm polytetrafluoroethylene (PTFE) filter, and the filter was washed with a mixture of ACN and water (1:1, v/v, 0.1% FA, 1 mL).

The filtrate was purified by RP-HPLC to give compound **12a** (101 mg, 32%) as a white solid. $^1\text{H NMR}$ (300 MHz, $\text{D}_2\text{O}/\text{CD}_3\text{CN} = 1:1$ (v/v)): δ 8.28 (d, $J = 8.5$ Hz, 2H), 7.98 (d, $J = 8.5$ Hz, 2H), 4.99 (q, $J = 2.9$ Hz, 1H), 4.67 (q, $J = 3.9$ Hz, 1H), 4.11 (dd, $J = 4.3$ and 14.5 Hz, 1H), 3.96 (dd, $J = 7.2$ and 14.5 Hz, 1H), 2.81 (t, $J = 7.4$ Hz, 2H), 2.57–2.44 (m, 1H), 2.35–2.21 (m, 1H); $^{13}\text{C NMR}$ (75 MHz, $\text{D}_2\text{O}/\text{CD}_3\text{CN} = 1:1$ (v/v)): δ 176.3, 175.5, 173.0, 168.4, 164.8, 159.9, 138.3, 133.1, 129.4, 99.2, 55.0, 52.8, 40.9, 30.4, 27.1. ESI-HRMS (m/z): calcd for $\text{C}_{16}\text{H}_{17}\text{IN}_3\text{O}_8^-$ [$\text{M} - \text{H}$] $^-$, 506.0066; found, 506.0064. >97% purity (as determined by RP-HPLC, method A, $t_{\text{R}} = 6.62$ min, method B, $t_{\text{R}} = 7.35$ min).

12b–12d were synthesized using a similar method as described for **12a**.

(*7S,12S*)-1-(4-Iodophenyl)-1,5,10-trioxo-2,6,9,11-tetraazatetradecane-7,12,14-tricarboxylic Acid (**12b**). This compound was obtained in 35% yield as a white solid, following the same procedure described for the synthesis of **12a** with 2,5-dioxopyrrolidin-1-yl 3-(4-iodobenzamido)propanoate instead of *N*-succinimidyl 4-iodobenzoate. $^1\text{H NMR}$ (300 MHz, D_2O): δ 7.85 (d, $J = 8.3$ Hz, 2H), 7.46 (d, $J = 8.3$ Hz, 2H), 4.51 (q, $J = 3.5$ Hz, 1H), 4.10 (q, $J = 3.5$ Hz, 1H), 3.73–3.59 (m, 3H), 3.47 (dd, $J = 6.8$ and 14.5 Hz, 1H), 2.62 (t, $J = 6.4$ Hz, 2H), 2.39 (t, $J = 7.3$ Hz, 2H), 2.12–1.99 (m, 1H), 1.89–1.75 (m, 1H); $^{13}\text{C NMR}$ (75 MHz, D_2O): δ 177.1, 176.1, 174.1, 173.3, 170.0, 165.0, 159.7, 137.9, 133.0, 128.6, 98.7, 53.5, 52.6, 40.5, 36.4, 35.2, 30.1, 26.2. ESI-HRMS (m/z): calcd for $\text{C}_{19}\text{H}_{21}\text{IN}_4\text{O}_9^-$ [$\text{M} - \text{H}$] $^-$, 577.0437; found, 577.0437. >97% purity (as determined by RP-HPLC, method A, $t_{\text{R}} = 6.16$ min, method B, $t_{\text{R}} = 8.20$ min).

(*8S,13S*)-1-(4-Iodophenyl)-1,6,11-trioxo-2,7,10,12-tetraazapentadecane-8,13,15-tricarboxylic Acid (**12c**). This compound was obtained in 56% yield as a white solid, following the same procedure described for the synthesis of **12a** with 2,5-dioxopyrrolidin-1-yl 4-(4-iodobenzamido)butanoate instead of *N*-succinimidyl 4-iodobenzoate. $^1\text{H NMR}$ (300 MHz, D_2O): δ 8.35 (d, $J = 8.4$ Hz, 2H), 8.09 (d, $J = 8.4$ Hz, 2H), 4.96 (dd, $J = 4.6$ and 7.2 Hz, 1H), 4.76–4.72 (m, 1H), 4.12 (dd, $J = 4.6$ and 14.3 Hz, 1H), 4.02–3.90 (m, 1H), 3.89 (t, $J = 7.0$ Hz, 2H), 2.92 (t, $J = 7.5$ Hz, 2H), 2.86 (t, $J = 7.4$ Hz, 2H), 2.70–2.55 (m, 3H), 2.50–2.25 (m, 1H); $^{13}\text{C NMR}$ (75 MHz, $\text{D}_2\text{O}/\text{CD}_3\text{CN} = 1:1$ (v/v)): δ 176.5, 175.8, 175.5, 173.4, 168.8, 159.6, 138.3, 134.1, 129.4, 98.7, 53.8, 52.9, 40.9, 39.6, 33.4, 30.5, 27.2, 25.3. ESI-HRMS (m/z): calcd for $\text{C}_{20}\text{H}_{25}\text{IN}_4\text{O}_9^-$ [$\text{M} - \text{H}$] $^-$, 591.0593; found, 591.0593. >97% purity (as determined by RP-HPLC, method A, $t_{\text{R}} = 7.32$ min, method B, $t_{\text{R}} = 9.37$ min).

(*9S,14S*)-1-(4-Iodophenyl)-1,7,12-trioxo-2,8,11,13-tetraazahexadecane-9,14,16-tricarboxylic Acid (**12d**). This compound was obtained in 22% yield as a white solid, following the same procedure described for the synthesis of **12a** with 2,5-dioxopyrrolidin-1-yl 5-(4-iodobenzamido)pentanoate instead of *N*-succinimidyl 4-iodobenzoate. $^1\text{H NMR}$ (300 MHz, D_2O): δ 7.87 (d, $J = 8.5$ Hz, 2H), 7.47 (d, $J = 8.5$ Hz, 2H), 4.50 (dd, $J = 4.7$ and 7.1 Hz, 1H), 4.17 (d, $J = 5.1$ and 9.1 Hz, 1H), 3.63 (dd, $J = 4.6$ and 14.4 Hz, 1H), 3.46 (dd, $J = 7.4$ and 14.4 Hz, 1H), 3.40 (t, $J = 6.3$ Hz, 2H), 2.47–2.28 (m, 4H), 2.15–1.96 (m, 1H), 1.92–1.75 (m, 1H), 1.65 (br s, 4H); $^{13}\text{C NMR}$ (75 MHz, D_2O): δ 177.2, 176.7, 176.3, 173.8, 170.0, 137.9, 133.3, 128.6, 98.4, 53.5, 52.7, 44.4, 40.5, 39.5, 35.0, 30.1, 27.8, 26.4, 22.6. ESI-HRMS (m/z): calcd for $\text{C}_{21}\text{H}_{25}\text{IN}_4\text{O}_9^-$ [$\text{M} - \text{H}$] $^-$, 605.0750; found, 605.0752. >97% purity (as determined by RP-HPLC, method A, $t_{\text{R}} = 8.79$ min, method B, $t_{\text{R}} = 9.86$ min).

Typical Procedure for the Synthesis of (*S*)-2-(3-((*R*)-2-carboxy-2-(4-iodobenzamido)ethyl)ureido)pentanedioic Acid (13a**).** *N*-Succinimidyl 4-iodobenzoate (270 mg, 0.78 mmol) and (*S*)-2-(3-((*R*)-2-amino-2-carboxyethyl)ureido)pentanedioic acid **7** (175 mg, 0.51 mmol) were placed in an oven-dried 100 mL two-necked round-bottom flask that was then fitted with a rubber septum and three-way connected to a balloon filled with argon. The flask was flushed with argon and anhydrous DCM (2 mL), followed by triethylamine (700 μL , 5.05 mmol). The reaction mixture was stirred at room temperature for 2 h. The reaction mixture was filtered through a 0.45 μm PTFE filter, and the filter was washed with a mixture of ACN and water (1:1, v/v, 0.1% FA, 1 mL). The filtrate was purified by RP-HPLC to give compound **13a** (27.6 mg, 9%) as a white solid. $^1\text{H NMR}$ (300 MHz, $\text{D}_2\text{O}/\text{CD}_3\text{CN} = 1:1$ (v/v)): δ 8.30 (d, $J = 8.5$ Hz, 2H), 7.97 (d, $J = 8.5$ Hz, 2H), 4.98

(dd, $J = 4.5$ and 7.0 Hz, 1H), 4.63 (dd, $J = 5.1$ and 8.9 Hz, 1H), 4.08 (dd, $J = 4.6$ and 14.5 Hz, 2H), 4.00 (dd, $J = 7.1$ and 14.5 Hz, 1H), 2.75 (t, $J = 7.5$ Hz, 2H), 2.57–2.37 (m, 1H), 2.35–2.18 (m, 1H); ^{13}C NMR (75 MHz, $\text{D}_2\text{O}/\text{CD}_3\text{CN} = 1:1$ (v/v)): δ 176.5, 175.8, 173.3, 168.7, 159.9, 138.3, 133.0, 129.4, 99.3, 55.1, 52.9, 40.9, 30.4, 27.1. ESI-HRMS (m/z): calcd for $\text{C}_{16}\text{H}_{17}\text{IN}_3\text{O}_8^- [\text{M} - \text{H}]^-$, 506.0066; found, 506.0063. >99% purity (as determined by RP-HPLC, method A, $t_{\text{R}} = 6.35$ min, method B, $t_{\text{R}} = 8.06$ min).

13b–13d were synthesized using a similar method as described for **13a**.

(7R,12S)-1-(4-Iodophenyl)-1,5,10-trioxo-2,6,9,11-tetraazatetradecane-7,12,14-tricarboxylic Acid (13b). This compound was obtained in 30% yield as a white solid, following the same procedure described for the synthesis of **13a** with 2,5-dioxopyrrolidin-1-yl 3-(4-iodobenzamido)propanoate instead of *N*-succinimidyl 4-iodobenzoate. ^1H NMR (300 MHz, D_2O): δ 7.85 (d, $J = 8.3$ Hz, 2H), 7.45 (d, $J = 8.3$ Hz, 2H), 4.49 (dd, $J = 5.1$ and 6.0 Hz, 1H), 4.11 (dd, $J = 5.3$ and 8.8 Hz, 1H), 3.71–3.55 (m, 3H), 3.49 (dd, $J = 6.7$ and 14.5 Hz, 1H), 2.60 (t, $J = 6.1$ Hz, 2H), 2.41 (t, $J = 7.3$ Hz, 2H), 2.17–1.99 (m, 1H), 1.96–1.75 (m, 1H); ^{13}C NMR (75 MHz, D_2O): δ 177.2, 176.2, 174.1, 173.5, 170.1, 159.6, 137.9, 133.0, 128.6, 98.6, 53.5, 52.6, 40.4, 36.4, 35.2, 30.1, 26.3. ESI-HRMS (m/z): calcd for $\text{C}_{19}\text{H}_{21}\text{IN}_4\text{O}_9^- [\text{M} - \text{H}]^-$, 577.0437; found, 577.0431. >97% purity (as determined by RP-HPLC, method A, $t_{\text{R}} = 6.32$ min, method B, $t_{\text{R}} = 8.50$ min).

(8R,13S)-1-(4-Iodophenyl)-1,5,10-trioxo-2,6,9,11-tetraazatetradecane-7,12,14-tricarboxylic Acid (13c). This compound was obtained in 32% yield as a white solid, following the same procedure described for the synthesis of **13a** with 2,5-dioxopyrrolidin-1-yl 4-(4-iodobenzamido)butanoate instead of *N*-succinimidyl 4-iodobenzoate. ^1H NMR (300 MHz, D_2O): δ 7.86 (d, $J = 8.5$ Hz, 2H), 7.46 (d, $J = 8.5$ Hz, 2H), 4.45 (dd, $J = 4.9$ and 6.9 Hz, 1H), 4.17 (dd, $J = 5.2$ and 9.0 Hz, 1H), 3.57 (dd, $J = 4.9$ and 14.4 Hz, 1H), 3.47 (dd, $J = 7.0$ and 14.5 Hz, 1H), 3.40 (t, $J = 6.8$ Hz, 2H), 2.47–2.30 (m, 4H), 2.18–2.01 (m, 1H), 1.98–1.80 (m, 3H); ^{13}C NMR (75 MHz, D_2O): δ 177.3, 176.6, 175.9, 174.1, 170.0, 159.6, 137.9, 133.2, 128.6, 98.5, 53.9, 52.9, 40.6, 39.2, 33.0, 30.2, 26.4, 24.6. ESI-HRMS (m/z): calcd for $\text{C}_{20}\text{H}_{25}\text{IN}_4\text{O}_9^- [\text{M} - \text{H}]^-$, 591.0593; found, 591.0593. >97% purity (as determined by RP-HPLC, method A, $t_{\text{R}} = 7.19$ min, method B, $t_{\text{R}} = 9.24$ min).

(9R,14S)-1-(4-Iodophenyl)-1,7,12-trioxo-2,8,11,13-tetraazahexadecane-9,14,16-tricarboxylic Acid (13d). This compound was obtained in 18% yield as a white solid, following the same procedure described for the synthesis of **13a** with 2,5-dioxopyrrolidin-1-yl 5-(4-iodobenzamido)pentanoate instead of *N*-succinimidyl 4-iodobenzoate. ^1H NMR (300 MHz, D_2O): δ 7.89 (d, $J = 8.1$ Hz, 2H), 7.49 (d, $J = 8.0$ Hz, 2H), 4.45 (br s, 1H), 4.13 (br s, 1H), 3.60 (dd, $J = 4.4$ and 13.7 Hz, 1H), 3.48 (dd, $J = 7.0$ and 13.8 Hz, 1H), 3.39 (br s, 2H), 2.56–2.26 (m, 4H), 2.16–1.97 (m, 1H), 1.96–1.78 (m, 1H), 1.65 (br s, 4H); ^{13}C NMR (75 MHz, D_2O): δ 177.4, 176.7, 176.5, 174.5, 170.1, 159.6, 137.9, 133.3, 128.6, 98.4, 54.0, 53.0, 40.7, 39.5, 35.1, 30.2, 27.7, 26.4, 22.5. ESI-HRMS (m/z): calcd for $\text{C}_{21}\text{H}_{25}\text{IN}_4\text{O}_9^- [\text{M} - \text{H}]^-$, 605.0750; found, 605.0753. >97% purity (as determined by RP-HPLC, method A, $t_{\text{R}} = 9.10$ min, method B, $t_{\text{R}} = 10.29$ min).

Typical Procedure for the Synthesis of (S)-2-(3-((S)-3-Carboxy-3-(4-iodobenzamido)propyl)ureido)pentanedioic Acid (14a). *N*-Succinimidyl 4-iodobenzoate (128 mg, 0.29 mmol) and (S)-2-(3-((S)-3-amino-3-carboxypropyl)ureido)pentanedioic acid **9** (90 mg, 0.25 mmol) were placed in an oven-dried 100 mL two-necked round-bottom flask that was then fitted with a rubber septum and three-way connected to a balloon filled with argon. The flask was flushed with argon and anhydrous DCM (2 mL) was added, followed by triethylamine (300 μL , 2.15 mmol). The reaction mixture was stirred at room temperature for 2 h. The reaction mixture was filtered through a 0.45 μm PTFE filter, and the filter was washed with a mixture of ACN and water (1:1, v/v, 0.1% FA, 1 mL). The filtrate was purified by RP-HPLC to give compound **14a** (42.8 mg, 27%) as a white solid. ^1H NMR (300 MHz, D_2O): δ 7.90 (d, $J = 8.1$ Hz, 2H), 7.54 (d, $J = 8.2$ Hz, 2H), 4.61 (dd, $J = 4.7$ and 8.9 Hz, 1H), 4.18 (dd, $J = 5.1$ and 8.6 Hz, 1H), 3.45–3.31 (m, 1H), 3.31–3.13 (m, 1H), 2.41 (t, $J = 7.3$ Hz, 2H), 2.28–1.96 (m, 4H), 1.96–1.76 (m, 1H); ^{13}C NMR (75 MHz, D_2O): δ 177.3, 176.5, 175.7, 170.1, 159.6, 137.9, 132.5, 128.8, 99.0, 52.7, 51.5, 36.6,

30.7, 30.2, 26.4. ESI-HRMS (m/z): calcd for $\text{C}_{17}\text{H}_{19}\text{IN}_3\text{O}_8^- [\text{M} - \text{H}]^-$, 520.0222; found, 520.0220. >97% purity (as determined by RP-HPLC, method A, $t_{\text{R}} = 6.98$ min, method B, $t_{\text{R}} = 8.09$ min).

14b–14d were synthesized using a similar method as described for **14a**.

(7S,13S)-1-(4-Iodophenyl)-1,5,11-trioxo-2,6,10,12-tetraazapentadecane-7,13,15-tricarboxylic Acid (14b). This compound was obtained in 15% yield as a white solid, following the same procedure described for the synthesis of **14a** with 2,5-dioxopyrrolidin-1-yl 3-(4-iodobenzamido)propanoate instead of *N*-succinimidyl 4-iodobenzoate. ^1H NMR (300 MHz, D_2O): δ 7.88 (d, $J = 6.9$ Hz, 2H), 7.48 (d, $J = 6.9$ Hz, 2H), 4.48–4.28 (m, 1H), 4.28–4.11 (m, 1H), 3.83–3.56 (m, 2H), 3.19–2.99 (m, 2H), 2.74–2.54 (m, 2H), 2.53–2.34 (m, 2H), 2.28–2.07 (m, 1H), 2.07–1.89 (m, 2H), 1.89–1.69 (m, 1H); ^{13}C NMR (75 MHz, D_2O): δ 177.4, 176.5, 175.8, 174.1, 170.0, 159.4, 137.9, 133.0, 128.6, 98.6, 52.8, 50.8, 36.5, 36.2, 35.3, 30.9, 30.2, 26.5. ESI-HRMS (m/z): calcd for $\text{C}_{20}\text{H}_{25}\text{IN}_4\text{O}_9^- [\text{M} - \text{H}]^-$, 591.0593; found, 591.0593. >97% purity (as determined by RP-HPLC, method A, $t_{\text{R}} = 6.32$ min, method B, $t_{\text{R}} = 8.06$ min).

(8S,14S)-1-(4-Iodophenyl)-1,6,12-trioxo-2,7,11,13-tetraazahexadecane-8,14,16-tricarboxylic Acid (14c). This compound was obtained in 24% yield as a white solid, following the same procedure described for the synthesis of **14a** with 2,5-dioxopyrrolidin-1-yl 4-(4-iodobenzamido)butanoate instead of *N*-succinimidyl 4-iodobenzoate. ^1H NMR (300 MHz, D_2O): δ 7.91 (d, $J = 8.5$ Hz, 2H), 7.50 (d, $J = 8.5$ Hz, 2H), 4.33 (dd, $J = 4.7$ and 9.1 Hz, 1H), 4.23 (dd, $J = 5.1$ and 9.0 Hz, 1H), 3.43 (t, $J = 6.8$ Hz, 2H), 3.29–3.03 (m, 3H), 2.48 (t, $J = 7.3$ Hz, 2H), 2.41 (t, $J = 7.1$ Hz, 2H), 2.22–2.08 (m, 1H), 2.06–1.75 (m, 5H); ^{13}C NMR (75 MHz, D_2O): δ 177.3, 176.5, 176.1, 175.7, 170.1, 159.6, 137.9, 133.2, 128.6, 98.5, 52.7, 50.7, 46.7, 39.3, 36.3, 32.9, 30.9, 30.2, 24.5. ESI-HRMS (m/z): calcd for $\text{C}_{21}\text{H}_{25}\text{IN}_4\text{O}_9^- [\text{M} - \text{H}]^-$, 605.0750; found, 605.0751. >97% purity (as determined by RP-HPLC, method A, $t_{\text{R}} = 7.54$ min, method B, $t_{\text{R}} = 9.19$ min).

(9S,15S)-1-(4-Iodophenyl)-1,7,13-trioxo-2,8,12,14-tetraazahexadecane-9,15,17-tricarboxylic Acid (14d). This compound was obtained in 28% yield as a white solid, following the same procedure described for the synthesis of **14a** with 2,5-dioxopyrrolidin-1-yl 5-(4-iodobenzamido)pentanoate instead of *N*-succinimidyl 4-iodobenzoate. ^1H NMR (300 MHz, D_2O): δ 7.89 (d, $J = 8.5$ Hz, 2H), 7.48 (d, $J = 8.5$ Hz, 2H), 4.33 (dd, $J = 4.4$ and 9.5 Hz, 1H), 4.14 (dd, $J = 5.0$ and 8.8 Hz, 1H), 3.38 (t, $J = 5.8$ Hz, 2H), 3.28–3.02 (m, 2H), 2.43 (t, $J = 7.3$ Hz, 2H), 2.35 (t, $J = 5.9$ Hz, 2H), 2.19–1.97 (m, 2H), 1.97–1.77 (m, 2H), 1.66 (br s, 4H); ^{13}C NMR (150 MHz, D_2O): δ 175.9, 175.7, 175.7, 175.6, 169.6, 159.0, 137.4, 133.1, 128.1, 97.7, 57.4, 56.0, 39.1, 36.4, 34.9, 31.4, 28.9, 27.7, 27.4, 22.3. ESI-HRMS (m/z): calcd for $\text{C}_{22}\text{H}_{28}\text{IN}_4\text{O}_9^- [\text{M} - \text{H}]^-$, 619.0906; found, 619.0905. >97% purity (as determined by RP-HPLC, method A, $t_{\text{R}} = 8.74$ min, method B, $t_{\text{R}} = 10.00$ min).

Typical Procedure for the Synthesis of (S)-2-(3-((R)-3-carboxy-3-(4-iodobenzamido)propyl)ureido)pentanedioic Acid (15a). *N*-Succinimidyl 4-iodobenzoate (65 mg, 0.19 mmol) and (S)-2-(3-((R)-3-amino-3-carboxypropyl)ureido)pentanedioic acid **11** (50 mg, 0.17 mmol) were placed in an oven-dried 100 mL two-necked round-bottom flask that was then fitted with a rubber septum and three-way connected to a balloon filled with argon. The flask was flushed with argon and anhydrous DCM (2 mL) was added, followed by triethylamine (700 μL , 5.05 mmol). The reaction mixture was stirred at room temperature for 2 h. The reaction mixture was filtered through a 0.45 μm PTFE filter, and the filter was washed with a mixture of ACN and water (1:1, v/v, 0.1% FA, 1 mL). The filtrate was purified by RP-HPLC to give compound **15a** (13.3 mg, 15%) as a white solid. ^1H NMR (300 MHz, D_2O): δ 7.90 (d, $J = 8.4$ Hz, 2H), 7.53 (d, $J = 8.4$ Hz, 2H), 4.57 (dd, $J = 4.5$ and 9.2 Hz, 1H), 4.16 (dd, $J = 5.2$ and 8.9 Hz, 1H), 3.29 (t, $J = 6.2$ Hz, 2H), 2.40 (t, $J = 7.4$ Hz, 2H), 2.30–1.98 (m, 3H), 1.98–1.78 (m, 1H); ^{13}C NMR (150 MHz, D_2O): δ 177.4, 176.7, 176.1, 170.1, 159.6, 137.9, 132.6, 128.8, 98.9, 52.9, 51.8, 36.6, 30.8, 30.2, 26.5. ESI-HRMS (m/z): calcd for $\text{C}_{17}\text{H}_{19}\text{IN}_3\text{O}_8^- [\text{M} - \text{H}]^-$, 520.0222; found, 520.0221. >97% purity (as determined by RP-HPLC, method A, $t_{\text{R}} = 7.29$ min, method B, $t_{\text{R}} = 8.17$ min).

15b–15d were synthesized using a similar method as described for **15a**.

(*7R,13S*)-1-(4-Iodophenyl)-1,5,11-trioxo-2,6,10,12-tetraazapentadecane-7,13,15-tricarboxylic Acid (**15b**). This compound was obtained in 44% yield as a white solid, following the same procedure described for the synthesis of **15a** with 2,5-dioxopyrrolidin-1-yl 3-(4-iodobenzamido)propanoate instead of *N*-succinimidyl 4-iodobenzoate. ¹H NMR (600 MHz, D₂O): δ 7.85 (d, *J* = 8.7 Hz, 2H), 7.46 (d, *J* = 8.7 Hz, 2H), 4.35 (dd, *J* = 4.5 and 9.0 Hz, 1H), 4.16 (dd, *J* = 5.4 and 8.8 Hz, 1H), 3.81–3.67 (m, 1H), 3.68–3.55 (m, 1H), 3.20–2.91 (m, 3H), 2.74–2.51 (m, 3H), 2.44 (t, *J* = 7.9 Hz, 3H), 2.20–2.05 (m, 1H), 2.05–1.86 (m, 3H), 1.88–1.71 (m, 1H); ¹³C NMR (150 MHz, D₂O): δ 177.4, 176.7, 176.1, 174.0, 169.9, 159.4, 137.9, 132.9, 128.6, 98.6, 52.9, 50.9, 36.5, 36.2, 35.2, 31.0, 30.2, 26.5. ESI-HRMS (*m/z*): calcd for C₂₀H₂₅N₄O₉[−] [M − H][−], 591.0593; found, 591.0596. >98% purity (as determined by RP-HPLC, method A, *t*_R = 5.99 min, method B, *t*_R = 7.75 min).

(*8R,14S*)-1-(4-Iodophenyl)-1,6,12-trioxo-2,7,11,13-tetraazahexadecane-8,14,16-tricarboxylic Acid (**15c**). This compound was obtained in 31% yield as a white solid, following the same procedure described for the synthesis of **15a** with 2,5-dioxopyrrolidin-1-yl 4-(4-iodobenzamido)butanoate instead of *N*-succinimidyl 4-iodobenzoate. ¹H NMR (300 MHz, D₂O): δ 8.24 (d, *J* = 8.1 Hz, 2H), 8.00 (d, *J* = 7.9 Hz, 2H), 4.73–4.61 (m, 1H), 4.61–4.42 (m, 1H), 3.72 (t, *J* = 6.6 Hz, 2H), 3.64–3.30 (m, 2H), 2.78 (t, *J* = 7.2 Hz, 2H), 2.70 (t, *J* = 7.4 Hz, 2H), 2.55–2.29 (m, 2H), 2.29–2.07 (m, 4H); ¹³C NMR (150 MHz, D₂O/CD₃CN = 1:1 (v/v)): δ 176.8, 176.1, 175.7, 175.4, 169.1, 159.5, 138.2, 133.8, 129.1, 98.7, 52.8, 50.8, 39.5, 36.6, 33.1, 31.4, 30.4, 26.9, 25.1. ESI-HRMS (*m/z*): calcd for C₂₁H₂₅N₄O₉[−] [M − H][−], 605.0750; found, 605.0758. >97% purity (as determined by RP-HPLC, method A, *t*_R = 7.55 min, method B, *t*_R = 9.23 min).

(*9R,15S*)-1-(4-Iodophenyl)-1,7,13-trioxo-2,8,12,14-tetraazahexadecane-9,15,17-tricarboxylic Acid (**15d**). This compound was obtained in 19% yield as a white solid, following the same procedure described for the synthesis of **15a** with 2,5-dioxopyrrolidin-1-yl 5-(4-iodobenzamido)pentanoate instead of *N*-succinimidyl 4-iodobenzoate. ¹H NMR (300 MHz, D₂O): δ 7.86 (d, *J* = 8.3 Hz, 2H), 7.46 (d, *J* = 8.3 Hz, 2H), 4.35 (dd, *J* = 4.5 and 9.5 Hz, 1H), 4.15 (q, *J* = 5.2 and 8.8 Hz, 1H), 3.38 (t, *J* = 5.7 Hz, 2H), 3.29–3.04 (m, 2H), 2.43 (t, *J* = 7.3 Hz, 2H), 2.35 (t, *J* = 6.8 Hz, 2H), 2.19–1.98 (m, 2H), 1.97–1.77 (m, 2H), 1.66 (br s, 4H); ¹³C NMR (75 MHz, D₂O): δ 177.4, 176.8, 176.7, 176.2, 170.1, 159.5, 137.9, 133.3, 128.6, 98.4, 52.9, 50.8, 44.5, 39.6, 36.3, 35.1, 31.0, 30.3, 27.8, 26.5. ESI-HRMS (*m/z*): calcd for C₂₂H₂₈N₄O₉[−] [M − H][−], 619.0906; found, 619.0909. >97% purity (as determined by RP-HPLC, method A, *t*_R = 8.76 min, method B, *t*_R = 10.08 min).

(*R*)-6-((*tert*-butoxycarbonyl)amino)-2-(3-((*S*)-1,5-di-*tert*-butoxy-1,5-dioxopentane-2-yl)ureido)hexanoic Acid (**16**). *L*-Glutamic acid di-*tert*-butyl ester hydrochloride (400 mg, 1.40 mmol) and triethylamine (1.4 mL, 10.9 mmol) were dissolved in anhydrous dichloromethane (5 mL). The solution was cooled to −78 °C under argon atmosphere. Triphosgene (128 mg, 0.40 mmol) was dissolved in anhydrous dichloromethane (3 mL) and added dropwise to the solution. The reaction mixture was slowly warmed up to room temperature and stirred for 30 min. *N*^ε-Boc-D-lysine (278 mg, 1.10 mmol) and triethylamine (1.3 mL, 9.0 mmol) dissolved in anhydrous DCM (5 mL) were added in the reaction mixture and stirred at room temperature for 24 h. The organic layer was washed with 3 N HCl and dried over MgSO₄. After removing the excess solvent under reduced pressure, the residue was purified by column chromatography on silica gel with DCM–methanol (100:1 to 30:1, v/v) to afford compound **16** in 52% yield (315 mg, 0.6 mmol). ¹H NMR (600 MHz, (CD₃)₂SO): δ 4.08–4.02 (m, 1H), 4.02–3.95 (m, 1H), 2.91–2.81 (m, 2H), 2.29–2.12 (m, 2H), 1.90–1.80 (m, 1H), 1.73–1.59 (m, 2H), 1.53–1.46 (m, 1H), 1.40 (s, 9H), 1.39 (s, 9H), 1.36 (s, 9H), 1.37–1.30 (m, 1H), 1.27–1.17 (m, 2H); ¹³C NMR (150 MHz, (CD₃)₂SO): δ 172.6, 171.9, 157.5, 157.5, 156.0, 155.9, 80.9, 80.1, 77.7, 55.3, 53.6, 53.4, 52.8, 52.7, 52.5, 33.2, 31.4, 30.0, 29.8, 29.7, 28.8, 28.6, 28.4, 28.3, 28.3, 28.2, 28.1, 28.0, 28.0, 27.9, 22.9, 22.8. ESI-HRMS (*m/z*): calcd for C₂₃H₄₅N₃O₉Na⁺ [M + Na]⁺, 554.3048; found, 554.3036.

(*S*)-2-(3-((*R*)-1-Carboxy-5-(4-iodobenzamido)pentyl)ureido)pentanedioic Acid (**17**). To a solution of **16** (215 mg, 0.4 mmol) in anhydrous DCM (8 mL) was added TFA (2 mL) at 0 °C. The reaction mixture was stirred at room temperature for 2 h and was concentrated under reduced pressure. The residue was washed by methanol three times and purged with argon gas. Without further purification, the residue was then dissolved in anhydrous DMF (2 mL). *N*-Succinimidyl 4-iodobenzoate (171 mg, 0.5 mmol) and triethylamine (440 μL, 3.2 mmol) were added to the reaction mixture dropwise. The reaction mixture was stirred at room temperature for 2.5 h and purified with RP-HPLC using 0.1% FA in water(A)/ACN(B). (The solvent gradient: 75% A from 0 to 10 min, 75% A to 70% A from 10 to 15 min, 70% A from 15 to 28 min at 2 mL/min flow rate). Compound **17** was obtained as a white solid (92 mg, 0.2 mmol) in 42% yield. ¹H NMR (600 MHz, CD₃OD): δ 7.85 (d, *J* = 8.5 Hz, 2H), 7.59 (d, *J* = 8.5 Hz, 2H), 4.31 (br s, 2H), 3.39 (t, *J* = 7.1 Hz, 2H), 2.45–2.32 (m, 2H), 2.19–2.10 (m, 1H), 1.97–1.85 (m, 2H), 1.78–1.60 (m, 3H), 1.54–1.43 (m, 2H); ¹³C NMR (150 MHz, CD₃OD): δ 175.1, 168.0, 158.6, 137.5, 134.0, 128.6, 97.6, 52.7, 39.4, 32.0, 29.8, 28.6, 27.7, 22.6. ESI-HRMS (*m/z*): calcd for C₁₉H₂₄IN₃O₈Na⁺ [M + Na]⁺, 572.0500; found, 572.0508.

NAALADase Assay. PSMA inhibitory activity of the final compounds was determined using a fluorescence-based assay according to a previously reported procedure.^{39,40} LNCaP cell extracts were prepared by disrupting cell membrane sonication in Tris buffer (50 mM Tris [pH 7.4] and 0.5% Triton X-100). The cell lysates of LNCaP cell extracts were incubated with the synthesized compounds in the presence of 1 μM *N*-acetylaspartylglutamate. The amount of reduced glutamate was measured using the Amplex Red glutamic acid kit (Molecular Probes Inc., Eugene, OR). The fluorescence was measured with a Cytation 5 Image Reader (BioTek Instruments Inc., Winooski, VT) with excitation at 545 nm and emission at 590 nm. Assays were performed in triplicate. Data analysis was performed using GraphPad Prism 7.00 (GraphPad Software, San Diego, CA). Inhibition curves were determined using semilog plots, and IC₅₀ values were determined at the concentration at which enzyme activity was inhibited by 50%. Statistical significance was determined by 95% confidence interval on GraphPad Prism.

Crystallization and Data Collection. Diffracting crystals of rhPSMA/inhibitor complexes were obtained using procedures described previously.⁴⁶ Briefly, rhPSMA (10 mg/mL) was mixed with a 50 mM stock solution of a given inhibitor in water (neutralized with NaOH) at the 1:20 molar ratio and the rhPSMA/inhibitor solution was then combined with an equal volume of the reservoir solution (32% pentaerythritol propoxylate, Sigma), 2% polyethylene glycol 3350 (Sigma), and 100 mM Tris-HCl, (pH 8.0). Diffraction quality crystals were grown using the hanging-drop vapor-diffusion setup at 293 K. The monocrystals of rhPSMA/inhibitor complexes were vitrified in liquid nitrogen directly from crystallization droplets, and the diffraction intensities for each complex were collected at 90 K using synchrotron radiation at the MX 14.2 beamline (BESSYII, Helmholtz-Zentrum Berlin, Germany; 0.91841 Å) equipped with a PILATUS 2M detector (Dectris, Switzerland). The complete data set for each complex was collected from a single crystal, and data were processed using XDSAPP.⁴⁷ The final data collection statistics are shown in Table 2.

Structure Determination, Refinement, and Analysis. Difference Fourier methods were used to determine the structures of PSMA/inhibitor complexes with ligand-free PSMA (PDB code 2OOT) used as a starting model.⁴⁶ Calculations were performed using Refmac 5.8., and the refinement protocol was interspersed with manual corrections to the model employing the program Coot 0.8.9.⁴⁸ The AceDRG program was used to generate restraint library and coordinate files for individual inhibitors.⁴⁹ Inhibitors were fitted into the positive electron density map in the final stages of the refinement. Approximately 2,000 of the randomly selected reflections were kept aside for cross-validation (*R*_{free}) during the refinement process. The quality of the final models was evaluated using the MOLPROBITY⁵⁰ and the relevant statistics are summarized in Table 2.

■ ASSOCIATED CONTENT

SI Supporting Information

The Supporting Information is available free of charge at <https://pubs.acs.org/doi/10.1021/acs.jmedchem.9b02022>.

Synthetic methods of the 4-iodobenzoate NHS esters with various lengths; analytical data (^1H - and ^{13}C NMR spectra, HPLC purity, and HRMS) of new compounds **12a–12d**, **13a–13d**, **14a–14d**, **15a–15d**, and **17**, and HPLC spectrograms for DCIBzL diastereoisomers (**2** and **17**) (PDF)

Binding pose of **13c** (PDB ID: 6RBC) in the active site of PSMA (PDB)

Binding pose of **14b** (PDB ID: 6S1X) in the active site of PSMA (PDB)

Molecular formula strings and biological data for final compounds (CSV)

Accession Codes

Coordinates and structure factors have been deposited in the Protein Data Bank (PDB) under accession codes 6RBC (PSMA with **13c**), 6S1X (PSMA with **14b**). The authors will release the atomic coordinates and experimental data upon article publication.

■ AUTHOR INFORMATION

Corresponding Authors

Xing Yang – Department of Nuclear Medicine, Peking University First Hospital, Beijing 100034, China; orcid.org/0000-0001-5186-4990; Phone: 86 10 83572928; Email: yangxing2017@bjmu.edu.cn

Zsofia Kutil – Institute of Biotechnology of the Czech Academy of Sciences, BIOCEV, 252 50 Vestec, Czech Republic; Phone: +420-325-873-736; Email: zsofia.kutil@ibt.cas.cz

Youngjoo Byun – College of Pharmacy, Korea University, Sejong 30019, Republic of Korea; Biomedical Research Center, Korea University Guro Hospital, Seoul 08308, Republic of Korea; orcid.org/0000-0002-0297-7734; Phone: +82-44-860-1619; Email: yjbyun1@korea.ac.kr; Fax: +82-44-860-1607

Authors

Kyul Kim – College of Pharmacy, Korea University, Sejong 30019, Republic of Korea

Hongmok Kwon – College of Pharmacy, Korea University, Sejong 30019, Republic of Korea

Cyril Barinka – Institute of Biotechnology of the Czech Academy of Sciences, BIOCEV, 252 50 Vestec, Czech Republic; orcid.org/0000-0003-2751-3060

Lucia Motlova – Institute of Biotechnology of the Czech Academy of Sciences, BIOCEV, 252 50 Vestec, Czech Republic

Sangjin Nam – College of Pharmacy, Korea University, Sejong 30019, Republic of Korea

Doyoung Choi – College of Pharmacy, Korea University, Sejong 30019, Republic of Korea

Hyunsoo Ha – College of Pharmacy, Korea University, Sejong 30019, Republic of Korea

Hwanhee Nam – Russell H. Morgan Department of Radiology and Radiological Science, Johns Hopkins University School of Medicine, Baltimore 21205, Maryland, United States

Sang-Hyun Son – College of Pharmacy, Korea University, Sejong 30019, Republic of Korea; orcid.org/0000-0002-8624-078X

Il Minn – Russell H. Morgan Department of Radiology and Radiological Science, Johns Hopkins University School of Medicine, Baltimore 21205, Maryland, United States

Martin G. Pomper – Russell H. Morgan Department of Radiology and Radiological Science, Johns Hopkins University School of Medicine, Baltimore 21205, Maryland, United States; orcid.org/0000-0001-6753-3010

Complete contact information is available at:

<https://pubs.acs.org/10.1021/acs.jmedchem.9b02022>

Author Contributions

K.K. and H.K. contributed equally. M.G.P., X.Y., and Y.B. designed the project. K.K., H.K., S.N., D.C., H.H., and S.-H.S. synthesized and analyzed the PSMA-targeted inhibitors. H.N. and I.M. performed the NAALADase assay. Z.K. and C.B. refined the X-ray crystal structures. L.M. crystallized the PSMA/inhibitor complexes and collected the crystallographic data. K.K., H.K., C.B., S.-H.S., M.G.P., X.Y., Z.K., and Y.B. analyzed the data and wrote the paper. All authors contributed to editing the final manuscript.

Notes

The authors declare no competing financial interest.

■ ACKNOWLEDGMENTS

The authors acknowledge Petra Baranova for the excellent technical assistance and the Helmholtz-Zentrum Berlin for the allocation of synchrotron radiation beamtime at the MX 14.2 beamline and funding from the CALIPSOplus under the grant agreement no. 730872 from the EU Framework Programme for Research and Innovation HORIZON 2020. This work was supported by the National Research Foundation of Korea (2017R1A2B4005036 and 2019R1A6A1A03031807 to Y.B.) and Ministry of Health & Welfare, Republic of Korea (HI16C1827 to Y.B.), the CAS (RVO: 86652036), Czech Science Foundation (19-22269Y), and the project and BIOCEV (CZ.1.05/1.1.00/02.0109) from the ERDF, and National Nature Science Foundation of China (NSFC 21877004).

■ ABBREVIATIONS

ACN, acetonitrile; Boc, *tert*-butoxycarbonyl; Cbz, carboxybenzyloxy; DCM, dichloromethane; DMF, *N,N*-dimethylformamide; ESI, electrospray ionization; FA, formic acid; HRMS, high-resolution mass spectrometry; IC₅₀, half maximal inhibitory concentration; NAALADase, *N*-acetyl-L-aspartyl-L-glutamate peptidase; NHS, *N*-hydroxysuccinimide; NMR, nuclear magnetic resonance; *Ot*-Bu, *tert*-butyl ester; PCa, prostate cancer; PSMA, prostate-specific membrane antigen; PTFE, polytetrafluoroethylene; RP-HPLC, reverse-phase high-performance liquid chromatography; TFA, trifluoroacetic acid

■ REFERENCES

- (1) Siegel, R. L.; Miller, K. D.; Jemal, A. Cancer statistics, 2018. *Ca-Cancer J. Clin.* **2018**, *68*, 7–30.
- (2) Chang, A. J.; Autio, K. A.; Roach, M., 3rd; Scher, H. I. High-risk prostate cancer-classification and therapy. *Nat. Rev. Clin. Oncol.* **2014**, *11*, 308–323.
- (3) Chang, S. S. Overview of prostate-specific membrane antigen. *Rev. Urol.* **2004**, *6*, S13–S18.
- (4) Ghosh, A.; Heston, W. D. W. Tumor target prostate specific membrane antigen (PSMA) and its regulation in prostate cancer. *J. Cell. Biochem.* **2004**, *91*, 528–539.

- (5) Silver, D. A.; Pellicer, I.; Fair, W. R.; Heston, W. D.; Cordon-Cardo, C. Prostate-specific membrane antigen expression in normal and malignant human tissues. *Clin. Cancer Res.* **1997**, *3*, 81.
- (6) Bostwick, D. G.; Pacelli, A.; Blute, M.; Roche, P.; Murphy, G. P. Prostate specific membrane antigen expression in prostatic intra-epithelial neoplasia and adenocarcinoma: A study of 184 cases. *Cancer* **1998**, *82*, 2256–2261.
- (7) Rowe, S. P.; Gorin, M. A.; Pomper, M. G. Imaging of poststate-specific membrane antigen with small-molecule PET radiotracers: From the bench to advanced clinical applications. *Annu. Rev. Med.* **2019**, *70*, 461–477.
- (8) Lim, E. Prostate-specific membrane antigen in prostate cancer imaging and treatment. *Transl. Cancer Res.* **2018**, *7*, S676–S689.
- (9) Machulkin, A. E.; Ivanenkov, Y. A.; Aladinskaya, A. V.; Veselov, M. S.; Aladinskiy, V. A.; Beloglazkina, E. K.; Koteliansky, V. E.; Shakhbazyan, A. G.; Sandulenko, Y. B.; Majouga, A. G. Small-molecule PSMA ligands. Current state, SAR and perspectives. *J. Drug Targeting* **2016**, *24*, 679–693.
- (10) Cimadamore, A.; Cheng, M.; Santoni, M.; Lopez-Beltran, A.; Battelli, N.; Massari, F.; Galosi, A. B.; Scarpelli, M.; Montironi, R. New prostate cancer targets for diagnosis, imaging, and therapy: Focus on prostate-specific membrane antigen. *Front. Oncol.* **2018**, *8*, 653.
- (11) Arsenault, F.; Beauregard, J.-M.; Pouliot, F. Prostate-specific membrane antigen for prostate cancer theranostics: From imaging to targeted therapy. *Curr. Opin. Support. Palliat. Care* **2018**, *12*, 359–365.
- (12) Jackson, P. F.; Cole, D. C.; Slusher, B. S.; Stetz, S. L.; Ross, L. E.; Donzanti, B. A.; Trainor, D. A. Design, synthesis, and biological activity of a potent inhibitor of the neuropeptidase N-acetylated α -linked acidic dipeptidase. *J. Med. Chem.* **1996**, *39*, 619–622.
- (13) Liu, T.; Toriyabe, Y.; Kazak, M.; Berkman, C. E. Pseudoirreversible inhibition of prostate-specific membrane antigen by phosphoramidate peptidomimetics. *Biochemistry* **2008**, *47*, 12658–12660.
- (14) Majer, P.; Jackson, P. F.; Delahanty, G.; Grella, B. S.; Ko, Y.-S.; Li, W.; Liu, Q.; Maclin, K. M.; Poláková, J.; Shaffer, K. A.; Stoermer, D.; Vitharana, D.; Wang, E. Y.; Zakrzewski, A.; Rojas, C.; Slusher, B. S.; Wozniak, K. M.; Burak, E.; Limsakun, T.; Tsukamoto, T. Synthesis and biological evaluation of thiol-based inhibitors of glutamate carboxypeptidase II: Discovery of an orally active GCP II inhibitor. *J. Med. Chem.* **2003**, *46*, 1989–1996.
- (15) Emmett, L.; Willowson, K.; Violet, J.; Shin, J.; Blanksby, A.; Lee, J. Lutetium¹⁷⁷ PSMA radionuclide therapy for men with prostate cancer: A review of the current literature and discussion of practical aspects of therapy. *J. Med. Radiat. Sci.* **2017**, *64*, 52–60.
- (16) Kratochwil, C.; Afshar-Oromieh, A.; Kopka, K.; Haberkorn, U.; Giesel, F. L. Current status of prostate-specific membrane antigen targeting in nuclear medicine: Clinical translation of chelator containing prostate-specific membrane antigen ligands into diagnostics and therapy for prostate cancer. *Semin. Nucl. Med.* **2016**, *46*, 405–418.
- (17) Kularatne, S. A.; Zhou, Z.; Yang, J.; Post, C. B.; Low, P. S. Design, synthesis, and preclinical evaluation of prostate-specific membrane antigen targeted ^{99m}Tc-radioimaging agents. *Mol. Pharm.* **2009**, *6*, 790–800.
- (18) Ganguly, T.; Dannoon, S.; Hopkins, M. R.; Murphy, S.; Cahaya, H.; Blecha, J. E.; Jivan, S.; Drake, C. R.; Barinka, C.; Jones, E. F.; VanBrocklin, H. F.; Berkman, C. E. A high-affinity [¹⁸F]-labeled phosphoramidate peptidomimetic PSMA-targeted inhibitor for PET imaging of prostate cancer. *Nucl. Med. Biol.* **2015**, *42*, 780–787.
- (19) Dannoon, S.; Ganguly, T.; Cahaya, H.; Geruntho, J. J.; Galliher, M. S.; Beyer, S. K.; Choy, C. J.; Hopkins, M. R.; Regan, M.; Blecha, J. E.; Skultetyova, L.; Drake, C. R.; Jivan, S.; Barinka, C.; Jones, E. F.; Berkman, C. E.; VanBrocklin, H. F. Structure-activity relationship of ¹⁸F-labeled phosphoramidate peptidomimetic prostate-specific membrane antigen (PSMA)-targeted inhibitor analogues for PET imaging of prostate cancer. *J. Med. Chem.* **2016**, *59*, 5684–5694.
- (20) Barinka, C.; Byun, Y.; Dusich, C. L.; Banerjee, S. R.; Chen, Y.; Castanares, M.; Kozikowski, A. P.; Mease, R. C.; Pomper, M. G.; Lubkowsky, J. Interactions between human glutamate carboxypeptidase II and urea-based inhibitors: Structural characterization. *J. Med. Chem.* **2008**, *51*, 7737–7743.
- (21) Navrátil, M.; Ptáček, J.; Šácha, P.; Starková, J.; Lubkowsky, J.; Bařinka, C.; Konvalinka, J. Structural and biochemical characterization of the folyl-poly- γ -L-glutamate hydrolyzing activity of human glutamate carboxypeptidase II. *FEBS J.* **2014**, *281*, 3228–3242.
- (22) Barinka, C.; Hlouchova, K.; Rovenska, M.; Majer, P.; Dauter, M.; Hin, N.; Ko, Y.-S.; Tsukamoto, T.; Slusher, B. S.; Konvalinka, J.; Lubkowsky, J. Structural basis of interactions between human glutamate carboxypeptidase II and its substrate analogs. *J. Mol. Biol.* **2008**, *376*, 1438–1450.
- (23) Barinka, C.; Rovenská, M.; Mlcochová, P.; Hlouchová, K.; Plechanovová, A.; Majer, P.; Tsukamoto, T.; Slusher, B. S.; Konvalinka, J.; Lubkowsky, J. Structural insight into the pharmacophore pocket of human glutamate carboxypeptidase II. *J. Med. Chem.* **2007**, *50*, 3267.
- (24) Zhang, A. X.; Murelli, R. P.; Barinka, C.; Michel, J.; Cocleaza, A.; Jorgensen, W. L.; Lubkowsky, J.; Spiegel, D. A. A remote arene-binding site on prostate specific membrane antigen revealed by antibody-recruiting small molecules. *J. Am. Chem. Soc.* **2010**, *132*, 12711–12716.
- (25) Banerjee, S. R.; Foss, C. A.; Castanares, M.; Mease, R. C.; Byun, Y.; Fox, J. J.; Hilton, J.; Lupold, S. E.; Kozikowski, A. P.; Pomper, M. G. Synthesis and evaluation of technetium-99m- and rhenium-labeled inhibitors of the prostate-specific membrane antigen (PSMA). *J. Med. Chem.* **2008**, *51*, 4504–4517.
- (26) Kozikowski, A. P.; Nan, F.; Conti, P.; Zhang, J.; Ramadan, E.; Bzdega, T.; Wroblewska, B.; Neale, J. H.; Pshenichkin, S.; Wroblewski, J. T. Design of remarkably simple, yet potent urea-based inhibitors of glutamate carboxypeptidase II (NAALADase). *J. Med. Chem.* **2001**, *44*, 298–301.
- (27) Chen, Y.; Pullambhatla, M.; Foss, C. A.; Byun, Y.; Nimmagadda, S.; Senthambizhelvan, S.; Sgouros, G.; Mease, R. C.; Pomper, M. G. 2-(3-{1-Carboxy-5-[(6-[¹⁸F]fluoro-pyridine-3-carbonyl)-amino]-pentyl}-ureido)-pentanedioic acid, [¹⁸F]DCFPyL, a PSMA-based PET imaging agent for prostate cancer. *Clin. Cancer Res.* **2011**, *17*, 7645–7653.
- (28) Eder, M.; Schäfer, M.; Bauder-Wüst, U.; Hull, W.-E.; Wängler, C.; Mier, W.; Haberkorn, U.; Eisenhut, M. ⁶⁸Ga-complex lipophilicity and the targeting property of a urea-based PSMA inhibitor for PET imaging. *Bioconjugate Chem.* **2012**, *23*, 688–697.
- (29) Benešová, M.; Schäfer, M.; Bauder-Wüst, U.; Afshar-Oromieh, A.; Kratochwil, C.; Mier, W.; Haberkorn, U.; Kopka, K.; Eder, M. Preclinical evaluation of a Tailor-Made DOTA-conjugated PSMA inhibitor with optimized linker moiety for imaging and endoradiotherapy of prostate cancer. *J. Nucl. Med.* **2015**, *56*, 914–920.
- (30) Cardinale, J.; Schäfer, M.; Benešová, M.; Bauder-Wüst, U.; Leotta, K.; Eder, M.; Neels, O. C.; Haberkorn, U.; Giesel, F. L.; Kopka, K. Preclinical evaluation of ¹⁸F-PSMA-1007, a new prostate-specific membrane antigen ligand for prostate cancer imaging. *J. Nucl. Med.* **2017**, *58*, 425–431.
- (31) Kelly, J.; Amor-Coarasa, A.; Nikolopoulou, A.; Kim, D.; Williams, C., Jr.; Ponnala, S.; Babich, J. W. Synthesis and pre-clinical evaluation of a new class of high-affinity ¹⁸F-labeled PSMA ligands for detection of prostate cancer by PET imaging. *Eur. J. Nucl. Med. Mol. Imag.* **2017**, *44*, 647–661.
- (32) Kwon, H.; Son, S.-H.; Byun, Y. Prostate-specific membrane antigen (PSMA)-targeted radionuclide probes for imaging and therapy of prostate cancer. *Asian J. Org. Chem.* **2019**, *8*, 1588–1600.
- (33) Kopka, K.; Benešová, M.; Bařinka, C.; Haberkorn, U.; Babich, J. Glu-ureido-based inhibitors of prostate-specific membrane antigen: Lessons learned during the development of a novel class of low-molecular-weight theranostic radiotracers. *J. Nucl. Med.* **2017**, *58*, 17S–26S.
- (34) Wester, H.-J.; Schottelius, M. PSMA-targeted radiopharmaceuticals for imaging and therapy. *Semin. Nucl. Med.* **2019**, *49*, 302–312.
- (35) Will, L.; Sonni, I.; Kopka, K.; Kratochwil, C.; Giesel, F. L.; Haberkorn, U. Radiolabeled prostate-specific membrane antigen small-molecule inhibitors. *Q. J. Nucl. Med. Mol. Imag.* **2017**, *61*, 168–180.
- (36) Pillai, M. R. A.; Nanabala, R.; Joy, A.; Sasikumar, A.; Knapp, F. F. Radiolabeled enzyme inhibitors and binding agents targeting PSMA: Effective theranostic tools for imaging and therapy of prostate cancer. *Nucl. Med. Biol.* **2016**, *43*, 692–720.

- (37) Hauke, S.; Best, M.; Schmidt, T. T.; Baalman, M.; Krause, A.; Wombacher, R. Two-step protein labeling utilizing lipoic acid ligase and Sonogashira cross-coupling. *Bioconjugate Chem.* **2014**, *25*, 1632–1637.
- (38) Shell, T. A.; Mohler, D. L. Selective targeting of DNA for cleavage within DNA-histone assemblies by a spermine- $[\text{CpW}(\text{CO})_3\text{Ph}]_2$ conjugate. *Org. Biomol. Chem.* **2005**, *3*, 3091–3093.
- (39) Robinson, M. B.; Blakely, R. D.; Couto, R.; Coyle, J. T. Hydrolysis of the brain dipeptide N-acetyl-L-aspartyl-L-glutamate. Identification and characterization of a novel N-acetylated α -linked acidic dipeptidase activity from rat brain. *J. Biol. Chem.* **1987**, *262*, 14498–14506.
- (40) Banerjee, S. R.; Pullambhatla, M.; Byun, Y.; Nimmagadda, S.; Foss, C. A.; Green, G.; Fox, J. J.; Lupold, S. E.; Mease, R. C.; Pomper, M. G. Sequential SPECT and optical imaging of experimental models of prostate cancer with a dual modality inhibitor of the prostate-specific membrane antigen. *Angew. Chem., Int. Ed.* **2011**, *50*, 9167–9170.
- (41) Chen, Y.; Foss, C. A.; Mease, R. C.; Nimmagadda, S.; Fox, J. J.; Kozikowski, A. P.; Pomper, M. G. Synthesis, biodistribution, and experimental prostate tumor imaging of p- $[\text{I}^{125}]$ iodobenzoyl-lys-NH(CO)NH-glu. *J. Nucl. Med.* **2007**, *48*, 19P.
- (42) Olszewski, R. T.; Bukhari, N.; Zhou, J.; Kozikowski, A. P.; Wroblewski, J. T.; Shamimi-Noori, S.; Wroblewska, B.; Bzdega, T.; Vicini, S.; Barton, F. B.; Neale, J. H. NAAG peptidase inhibition reduces locomotor activity and some stereotypes in the PCP model of schizophrenia via group II mGluR. *J. Neurochem.* **2004**, *89*, 876–885.
- (43) Barinka, C.; Novakova, Z.; Hin, N.; Bím, D.; Ferraris, D. V.; Duvall, B.; Kabarriti, G.; Tsukamoto, R.; Budesinsky, M.; Motlova, L.; Rojas, C.; Slusher, B. S.; Rokob, T. A.; Rulíšek, L.; Tsukamoto, T. Structural and computational basis for potent inhibition of glutamate carboxypeptidase II by carbamate-based inhibitors. *Bioorg. Med. Chem.* **2019**, *27*, 255–264.
- (44) Wang, H.; Byun, Y.; Barinka, C.; Pullambhatla, M.; Bhang, H.-e. C.; Fox, J. J.; Lubkowski, J.; Mease, R. C.; Pomper, M. G. Bioisosterism of urea-based GCPII inhibitors: Synthesis and structure-activity relationship studies. *Bioorg. Med. Chem. Lett.* **2010**, *20*, 392–397.
- (45) Kelly, J. M.; Amor-Coarasa, A.; Nikolopoulou, A.; Wüstemann, T.; Barelli, P.; Kim, D.; Williams, C., Jr.; Zheng, X.; Bi, C.; Hu, B.; Warren, J. D.; Hage, D. S.; DiMagno, S. G.; Babich, J. W. Dual-target binding ligands with modulated pharmacokinetics for endoradiotherapy of prostate cancer. *J. Nucl. Med.* **2017**, *58*, 1442–1449.
- (46) Barinka, C.; Starkova, J.; Konvalinka, J.; Lubkowski, J. A high-resolution structure of ligand-free human glutamate carboxypeptidase II. *Acta Crystallogr., Sect. F: Struct. Biol. Cryst. Commun.* **2007**, *63*, 150–153.
- (47) Krug, M.; Weiss, M. S.; Heinemann, U.; Mueller, U. XDSAPP: A graphical user interface for the convenient processing of diffraction data using XDS. *J. Appl. Crystallogr.* **2012**, *45*, 568–572.
- (48) Emsley, P.; Lohkamp, B.; Scott, W. G.; Cowtan, K. Features and development of Coot. *Acta Crystallogr., Sect. D: Biol. Crystallogr.* **2010**, *66*, 486–501.
- (49) Long, F.; Nicholls, R. A.; Emsley, P.; Gražulis, S.; Merkys, A.; Vaitkus, A.; Murshudov, G. N. A stereochemical description generator for ligands. *Acta Crystallogr., Sect. D: Biol. Crystallogr.* **2017**, *73*, 112–122.
- (50) Chen, V. B.; Arendall, W. B., 3rd; Headd, J. J.; Keedy, D. A.; Immormino, R. M.; Kapral, G. J.; Murray, L. W.; Richardson, J. S.; Richardson, D. C. MolProbity: All-atom structure validation for macromolecular crystallography. *Acta Crystallogr., Sect. D: Biol. Crystallogr.* **2010**, *66*, 12–21.